iScience

Article

Metabolic and transcriptional regulation of reproductive diapause in *Arma chinensis*

Graphical abstract

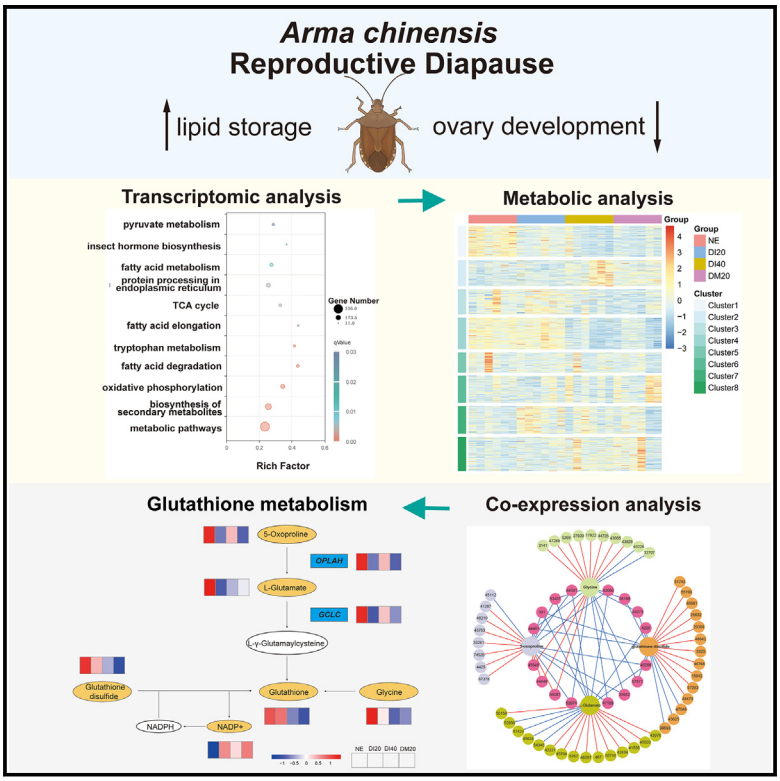

Highlights

- Metabolomic and transcriptomic profiling reveals stage-specific diapause regulation
- Glutathione metabolism links redox state to diapause progression
- Insulin signaling orchestrates metabolic reprogramming during diapause
- Energy metabolism shifts support enhanced survival in diapausing *A chinensis*

Authors

Maosen Zhang, Weiwei He, Yuyan Li, Junjie Chen, Nicholas M. Teets, Lisheng Zhang

Correspondence

liyuyan@caas.cn (Y.L.), zhangleesheng@163.com (L.Z.)

In brief

Entomology; Genetics; Omics

Zhang et al., 2025, iScience *28*, 111761
March 21, 2025
https://doi.org/10.1016/j.isci.2025.111761

CellPress

iScience

CellPress
OPEN ACCESS

Article

Metabolic and transcriptional regulation of reproductive diapause in *Arma chinensis*

Maosen Zhang,[1,4] Weiwei He,[1,4] Yuyan Li,[1,*] Junjie Chen,[1] Nicholas M. Teets,[3] and Lisheng Zhang[1,2,4,5,*]

[1]State Key Laboratory for Biology of Plant Diseases and Insect Pests, Key Laboratory of Natural Enemy Insects, Ministry of Agriculture and Rural Affairs, Institute of Plant Protection, Chinese Academy of Agricultural Sciences, Beijing 100193, P.R. China

[2]Key Laboratory of Animal Biosafety Risk Prevention and Control (North) of Ministry of Agriculture and Rural Affairs, Shanghai Veterinary Research Institute, Chinese Academy of Agricultural Sciences, Shanghai 200241, China

[3]Department of Entomology, University of Kentucky, Lexington, KY 40546, USA

[4]These authors contributed equally

[5]Lead contact

*Correspondence: liyuyan@caas.cn (Y.L.), zhangleesheng@163.com (L.Z.)

https://doi.org/10.1016/j.isci.2025.111761

SUMMARY

Diapause enables insects to survive unfavorable conditions through metabolic and developmental adjustments. We investigated metabolic regulation during reproductive diapause in the predatory stinkbug *Arma chinensis* using transcriptomic and metabolomic analyses. Our study revealed 9,254 differentially expressed genes and 493 significantly changed metabolites across diapause stages. Key metabolic pathways including glutathione metabolism, TCA cycle, glycolysis, and lipid metabolism underwent substantial reorganization. The pre-diapause phase showed increased energy consumption and lipid accumulation, while the maintenance phase exhibited restructuring of amino acid and glucose metabolism. We identified stage-specific metabolic signatures and potential regulatory mechanisms, including the roles of glutathione metabolism in redox regulation and insulin signaling in diapause control. This comprehensive characterization of metabolic reprogramming during *A. chinensis* diapause provides insights for improving biocontrol agent production and storage strategies.

INTRODUCTION

Entering a dormant state of diapause is an important survival strategy adopted by numerous insects, enabling them to survive unfavorable environmental conditions and thereby synchronize their life cycles with seasonally available resources.[1] Diapause is typically initiated by the perception of environmental cues and is tightly regulated by a combination of endocrine and molecular mechanisms.[2] It is a dynamic physiological process that encompasses three phases: pre-diapause (induction and preparation), diapause (initiation, maintenance, and termination) and post-diapause.[3] In general, diapause is characterized by developmental arrest, reduced metabolic rate, increased energy storage, and enhanced stress resistance.[4,5] Understanding the characteristics of insect diapause and its regulatory mechanisms will help to reveal the seasonal adaptive developmental mechanism of insects, predict insect population dynamics in nature, and improve the storage of beneficial insects through diapause manipulation.[6,7]

Metabolic suppression is a common feature of diapausing insects, as demonstrated in species like *Sarcophaga crassipalpis*, *Helicoverpa armigera*,[8,9] *Pilophorus gallicus*,[10] and *Pyrrhocoris apterus*.[11] This reduction in metabolism is typically accompanied by increased energy storage to ensure adequate energy reserves to survive winter.[12] The metabolic pathways and energy sources utilized by insects during diapause undergo significant changes from early to late stages.[13] The tricarboxylic acid (TCA) cycle, crucial for energy metabolism, is notably subdued during diapause as evidenced by studies on both *Sitodiplosis mosellana* and *Caenorhabditis elegans*. These studies reveal a reduction in TCA cycle activity, aligning with the organism's lowered metabolic state to endure environmental extremes.[14,15] Insects predominantly rely on lipids, amino acids, and carbohydrates as their primary energy sources during diapause. For instance, energy can be derived from serine and glycine for pyruvate synthesis.[16,17] Trehalose is a well-known metabolic energy source and cryoprotectant that is commonly elevated and during diapause of many insects, including *Nasonia vitripennis*,[18] *S. mosellana*, and *Mamestra brassicae*.[19,20] Triglycerides, mainly synthesized in adipose tissue due to their high caloric value and role in metabolic water storage, constitute the primary lipid component in insects and often accumulate during the induction and maintenance of diapause.[21,22] Acetyl-CoA carboxylase (*ACC*) and fatty acid synthase (*FAS*), two crucial genes in the fatty acid synthesis pathway, play a pivotal role in this process.[23,24] Moreover, changes in photoperiod can regulate the insulin signaling pathway, which, in turn, affects the upstream development of the reproductive system and fat metabolism.[25–27] Therefore, deciphering the molecular regulatory basis of diapause and cold tolerance is compelling for understanding the seasonal developmental adaptation and harnessing diapause for practical purposes.

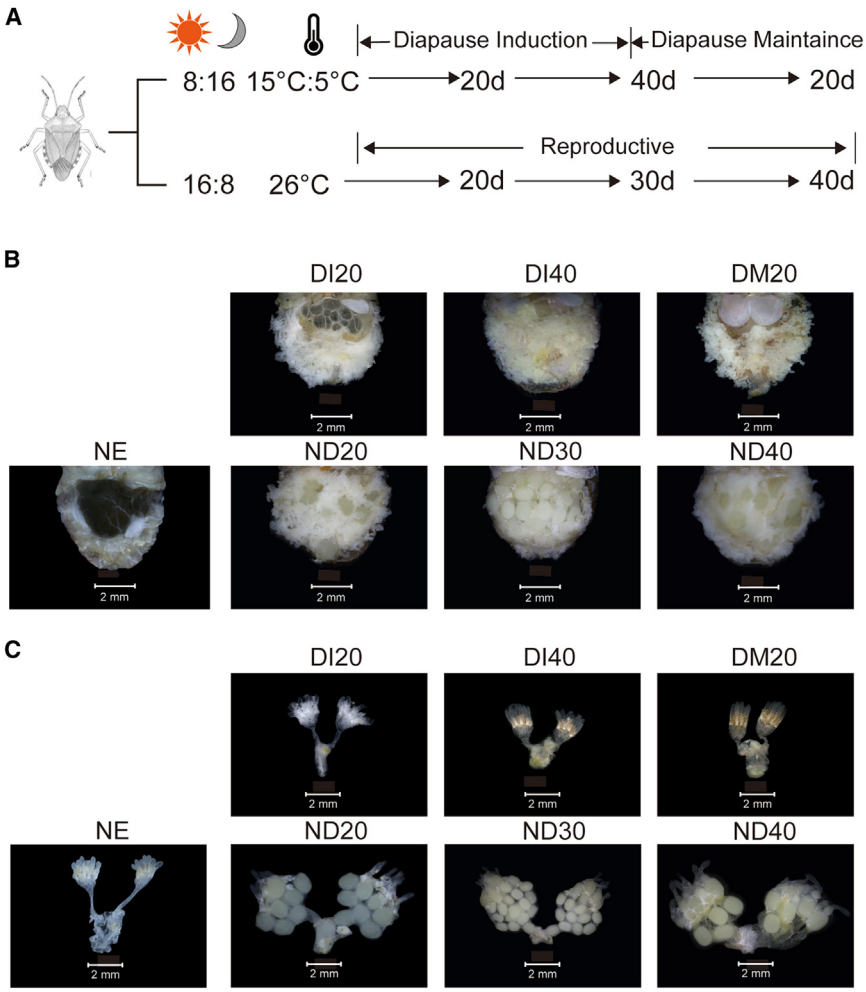

Figure 1. Sampling design and morphological changes during diapause in *A. chinensis*

(A) The sampling time points of *A. chinensis* female adults reared under diapause-inducing conditions (top) and normal developmental conditions (below).

(B) The abdominal fat accumulation state of diapause-destined females (DI20, DI40, and DM20) and normally developed females (ND20, ND30, and ND40). Abdominal observations were performed at 30x magnification.

(C) Ovarian development status of *A. chinensis* female adults reared under diapause-inducing conditions (DI20, DI40 and DM20) and normal developmental conditions (ND20, ND30, and ND40). Ovarian examinations were conducted at 50x magnification. Under diapause-inducing conditions, female adult ovarian development was inhibited, while normally developed female adults had high levels of yolk deposits and larger ovaries. Scale bars in all images represent 2 mm. Data are representative of at least 10 individuals examined per time point.

The predatory stinkbug *Arma chinensis* (Fallou) (Hemiptera: Pentatomidae) is an effective predatory stinkbug known for preying on many Lepidopteran and Coleopteran pests, including *Spodoptera frugiperda*, *Spodoptera litura*, *Leptinotarsa decemlineata*, and *Hyphantria cunea*.[28,29] As a biological control agent, this predator can be mass-reared on alternative prey, *Mythimna separata*, or an artificial diet, with an annual breeding capacity exceeding 70 million individuals in China. It has been widely used in the biological control of lepidopteran pests in greenhouse vegetables and tobacco fields, covering an annual application area exceeding 50,000 ha. To enhance the utilization of *A. chinensis*, extending its storage life is crucial, as it will facilitate mass production and enable large-scale release at the appropriate time as required in augmentative biological control of pests. The previous studies of our laboratory demonstrated that *A. chinensis* can enter a reproductive diapause state after being exposed to a thermoperiod with 8 h thermophase (15°C): 16 h cryophase (5°C) for 40 days, and the diapausing adult can be stored at these conditions for over 150 days, with a maximum storage duration of up to 300 days. Such a diapause feature in *A. chinensis* offers a unique developmental stage suitable for storage. Like other insects with reproductive diapause, the typical diapause characteristics of *A. chinensis* include suppression of feeding, mating, and reproduction, fat accumulation, and increased cold tolerance. During diapause, *A. chinensis* exhibits two key morphological characteristics: arrested ovarian development and significant abdominal fat accumulation (Figures 1B and 1C). However, the physiological and molecular basis that generates these diapause phenotypes in *A. chinensis* is still not clear.[27,30–33]

In this study, we explore metabolic and transcriptional regulation of diapause during induction and maintenance of diapause in *A. chinensis* by using a combined transcriptomic and metabolomic approach. Using RNA sequencing (RNA-seq), we simultaneously measure the expression of 43,017 transcripts in response to diapause. In addition, we tracked the levels of 797 metabolites at multiple time points during diapause using Quasi-targeted metabolomics based on liquid chromatography-tandem mass spectrometry (LC-MS/MS). Our results reveal the unique importance of biological processes associated with energy metabolism, amino acid metabolism, lipid metabolism, and hormonal signaling at different phases of diapause. Furthermore, we constructed an omics database to investigate the molecular mechanisms of diapause regulation, particularly to explore the functions of key genes and metabolites that specifically co-changed at the induction, initiation and duration of diapause.

RESULTS

Transcriptome profiles of *A. chinensis* in response to diapause

To quantify changes in gene expression in *A. chinensis* during the stages of diapause induction, initiation and maintenance,

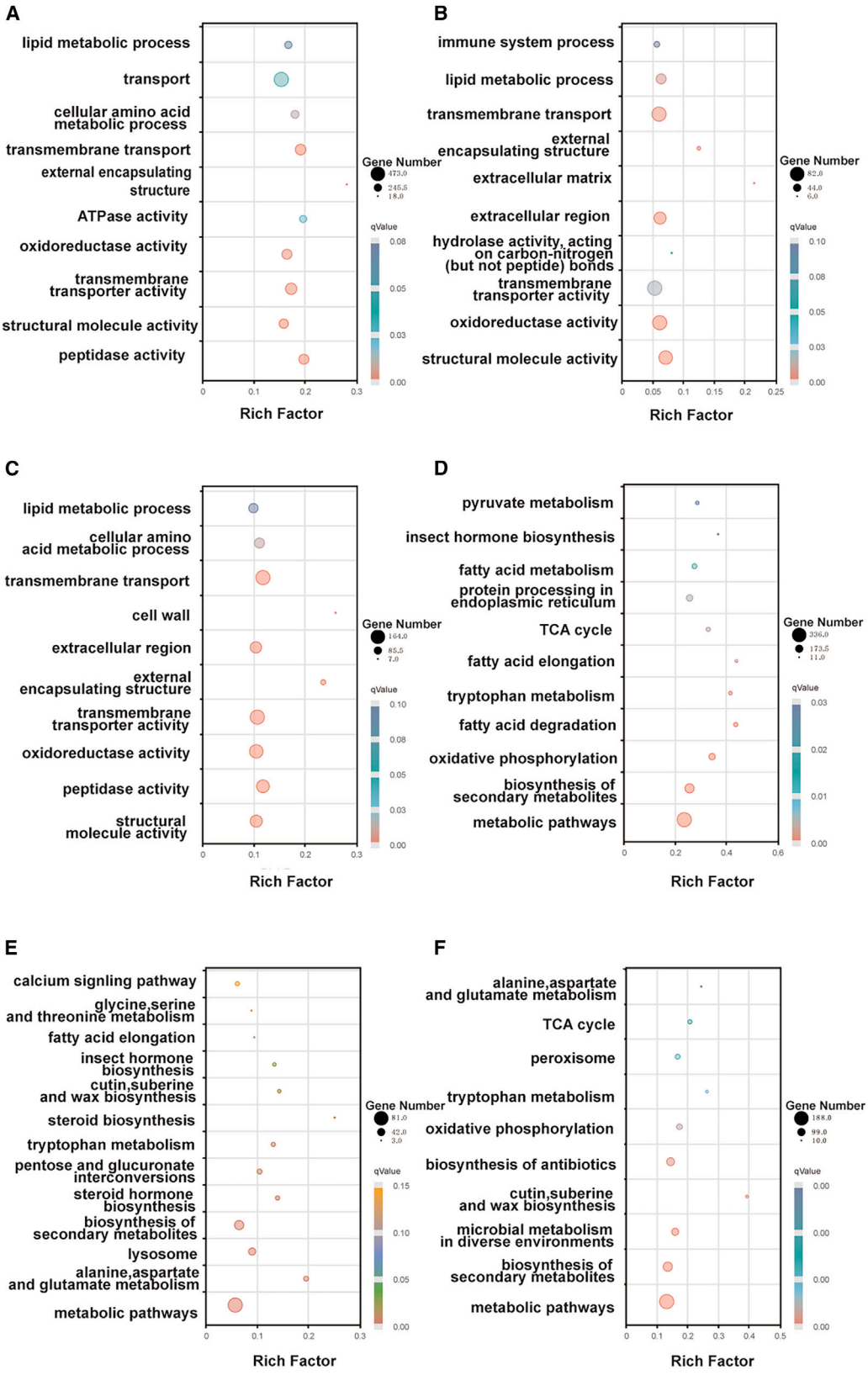

(legend on next page)

the transcriptome was sequenced using second-generation sequencing (Illumina RNA-seq) technology on the Illumina NovaSeq 6000 platform. A total of 263,620,024 clean reads were obtained after the low-quality reads were eliminated. With three biological replicates per time point, the 12 samples yielded 192 Gb high-quality data with the base percentage of Q30 score of 91.68%–93.66% and GC percentages of 35.27%–42.79% (Table S2). A total of 118,104 unique genes were obtained (Table S3). Based on the quantitative expression results, a differential expressed gene (DEG) analysis was performed, comparing the DI20, DI40, and DM20 groups with NE group, respectively. In total, 4,804 (1,734 up and 3,070 downregulated), 1,583 (655 up and 928 downregulated), and 2,867 (979 up and 1,888 downregulated) DEGs (|fold change|>2 and corrected padj<0.05) were obtained from the DI20, DI40, and DM20, respectively (Table S4).

The functional annotation and enrichment analysis of differentially expressed genes (DEGs) across various diapause stages were performed to elucidate the molecular mechanisms underlying diapause in *A. chinensis* (Figure 2). GO and KEGG analyses highlighted stage-specific molecular changes. In the DI20 vs. NE comparison group, lipid metabolic processes and pyruvate metabolism were significantly enriched (Figures 2A and 2D), suggesting a metabolic shift. The DI40 vs. NE comparison group showed prominent enrichment in transmembrane transport and pathways related to carbon metabolism and fatty acid elongation (Figures 2B and 2E), indicating ongoing metabolic adjustments. In the DM20 vs. NE comparison group, oxidoreductase activity and oxidative phosphorylation pathways were notably enriched (Figures 2C and 2F), reflecting adjustments in energy metabolism. The Rich Factor values and adjusted *p* values (*padj*) demonstrated the significance of these enrichments. The Rich Factor value of the horizontal coordinate in Figure 2 represents the ratio of differentially expressed genes to the total genes in a pathway, with higher values indicating greater enrichment. The padj values demonstrated the statistical significance of these enrichments.

To validate the transcriptome analysis, we performed quantitative real-time PCR on eight key genes involved in diapause regulation and lipid metabolism: *DR-2*, *JHAMT*, *PEBCK*, *ACC*, *FAS*, *tim*, *PK*, and *HK*. Figure S1 compares RNA-seq data (FPKM values, Figure S1A) with RT-qPCR results (relative expression levels, Figure S1B). The expression patterns observed in RT-qPCR closely mirrored those from RNA-seq. Genes such as *DR-2* and *HK* showed consistent upregulation during diapause progression, while *JHAMT* and *PEBCK* exhibited general downregulation in diapause stages compared to NE. Some genes (e.g., *ACC*, *FAS*) displayed more complex patterns, but these patterns were largely consistent between different methods.

Metabolomic alterations during diapause of *A. chinensis*

Shifts in metabolomes of *A. chinensis* during diapause induction and maintenance were determined using a quasi-targeted metabolomics approach based on LC-MS/MS. A total of 797 metabolites were identified in all samples. These metabolites belonged to 39 classes, including amino acid and its derivatives (163), fatty acyls (54), organic acid and its derivatives (117) etc. Key lipid-related metabolites such as gamma-nonanolactone, 20-carboxy-leukotriene B4, undecanedioic acid, erucic acid, stearic acid, linoleic acid, palmitoleic acid, and docosahexaenoic acid were identified, highlighting significant shifts in lipid synthesis, breakdown, and signaling pathways across different diapause stages. The PCA results demonstrate clear separation between diapause stages and non-diapause (NE) samples, indicating distinct metabolic profiles and effective grouping (Figure 3A). To identify the pivotal metabolites in *A. chinensis* during diapause, the differentially expressed metabolites (DEMs) were screened using the criteria of VIP >1.0, fold change FC > 1.2 or FC < 0.833, and *p* value <0.05. In the DI20 vs. NE comparison group, a total of 114 differential metabolites were identified (55 increased, 59 decreased); in the DI40 vs. NE comparison group, a total of 186 differential metabolites were identified (55 increased, 131 decreased); in the DM20 vs. NE comparison group, a total of 193 differential metabolites were annotated (58 increased, 135 decreased) (Figure 3B). Screening revealed that 18 metabolites were significantly different across all three comparison groups, including amino acids and their derivatives such as N-acetyl-D-mannosamine, 2,6-diaminoheptanedioic acid, 5-hydroxyproline, O-phosphotyrosine, glycine, S-adenosyl-L-methioninamine, and γ-glutamylglutamate; benzoic acid and its derivatives including 4-hydroxybenzoic acid; alcohols and their polyols including D-ribose-4-phosphate; glycerides including 1,3-diphosphoglycerate; phospholipids including lyso-phosphatidylethanolamine 18:2 and β-acetyl-γ-*O*-hexadecyl-L-α-lysophosphatidylcholine; sugars and their derivatives including glucose and β-D-glucose; organic acids and their derivatives including pyroglutamic acid, malic acid, 2-oxoadipic acid, and 2-aminoethyl phosphate. The hierarchical clustering analysis of metabolite abundances (Figure 3C) offered more granular insights. The resulting heatmap revealed distinct metabolite clusters with stage-specific abundance patterns across NE, DI20, DI40, and DM20 groups. This visualization allowed for the identification of metabolites that are uniquely up or downregulated in specific diapause stages, providing a detailed view of the metabolic shifts occurring during diapause progression that complement the broader patterns seen in the PCA.

To better understand the temporal patterns of metabolic changes during diapause, we performed k-means clustering analysis of all 797 identified metabolites. The optimal number of clusters (k = 8) was determined using the Silhouette Score Index (SSI) criterion, which showed the best balance between cluster separation and cohesion (Figure 3C). These eight clusters exhibited distinct expression patterns across different

Figure 2. Functional annotation and enrichment analysis of differentially expressed genes (DEGs) during diapause

(A–C) GO enrichment of DEGs in DI20vsNE (A), DI40vsNE (B), and DM20vsNE (C).

(D–F) KEGG pathway analysis of DEGs in DI20vsNE (D), DI40vsNE (E), and DM20vsNE (F). Dot size represents the number of DEGs in each term (Gene Number). Color indicates the adjusted *p* value (padj) of enrichment. The x axis shows the Rich Factor (ratio of DEGs to total genes in each term). Key enriched pathways and GO terms are labeled on the y axis. Pathways and terms are ordered by significance, with the most significant at the top of each plot. Data were obtained from three biological replicates per group.

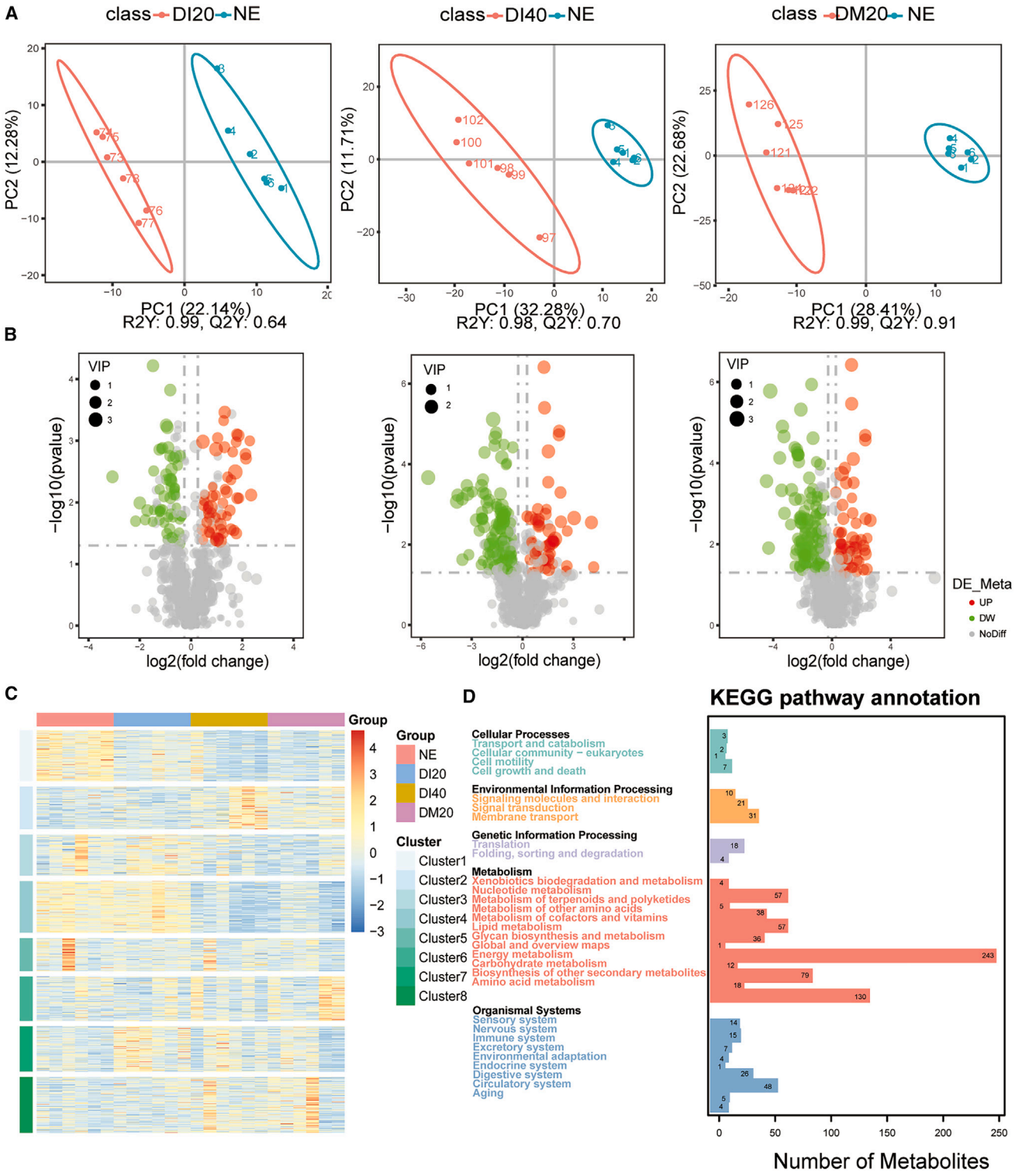

Figure 3. Multivariate analysis of metabolomic changes in *A. chinensis* at different times during diapause (20 [DI20], 40 [DI40] and 60 days [DM20] under diapause inducing conditions)

(A) Principal component analysis (PCA) of metabolome data derived from DI20, DI40, and DM20. Distinct clustering of diapause and non-diapause groups indicates significant metabolic differences. Ellipses represent 95% confidence intervals. Percentages on axes show the variance explained by each principal component.

(legend continued on next page)

phases of diapause. Notably, cluster 1 was enriched in carbohydrate-related metabolites, including various phosphorylated sugars and their derivatives. Clusters 2 and 3 contained numerous lipid-related compounds and amino acid derivatives, respectively, reflecting the metabolic reprogramming of energy storage during the pre-diapause phase. Clusters 4 and 5 were characterized by peptides, amino acids, and nucleotide metabolites, which showed distinct expression patterns during diapause maintenance. Clusters 6–8 comprised various organic acids, hormones, and small molecule metabolites involved in energy metabolism, suggesting active metabolic restructuring throughout the diapause process (Table S7). All DEMs were functionally annotated and subjected to pathway enrichment analysis using KEGG. Based on the biological functional hierarchy of the metabolites, KEGG compounds were classified into several categories, including cellular processes, environmental information processing, genetic information processing, metabolism and organismal systems. As shown in Figure 3D, the categories of metabolic and organismal systems were significantly enriched in all diapause-induced groups. More specifically, the top three significantly enriched pathways in the metabolism category were amino acid metabolism, carbohydrate metabolism, and nucleotide metabolism, while digestive system, endocrine system and nervous system were the top three in the organismal systems category. These differentially expressed metabolites (DEMs) were grouped into 37 species, which were mainly classified into fatty acyls (54), nucleotide and its derivates (86), carbohydrates and its derivatives (45), nucleotide and its derivates (163), organic acid and its derivatives (117), hormones (29) and others (Figure 3D; Tables S5 and S6).

Integrated analysis of the transcriptome and metabolome

To elucidate the intricate relationships between differentially expressed genes and metabolites during diapause progression in *A. chinensis*, we performed correlation heatmap analyses across three key stages: DI20 vs. NE, DI40 vs. NE, and DM20 vs. NE. *A. chinensis* at the diapause induction stage (DI20) exhibited distinct clusters of gene-metabolite correlations. The diapause initiation phase (DI40) maintained some correlations while new clusters emerged. The maintenance phase (DM20) displayed a markedly different correlation pattern, with weakening of some previously strong correlations and emergence of new ones. These dynamic shifts in correlation patterns reflect stage-specific metabolic adaptations in *A. chinensis* during diapause progression (Figures S3A–S3C).

A comprehensive correlation analysis was performed between the metabolomic and transcriptomic data of *A. chinensis* by using the cancor function from R. The screening criteria were as follows: Pearson correlation coefficient >0.8 and p *value* < 0.05. Correlation network analysis was performed on the top 5 differentially abundant metabolites from metabolomic enrichment and top 10 differentially expressed genes from transcriptomic analysis across different diapause stages in *A. chinensis*. These top metabolites and genes were selected based on their fold change and statistical significance, representing the most dramatically altered molecular components during diapause progression. In the DI20 vs. NE comparison, key metabolites included 5-oxoproline (glutathione metabolism), Thr-Leu (protein metabolism), *cis*-7-hexadecenoic acid (lipid metabolism), 2,6-diaminooimelic acid (lysine biosynthesis), and N-acetylmannosamine (glycoprotein synthesis). These metabolites exhibited significant correlations with the expression of genes such as pro-resilin (cuticle elasticity), copine-4 (membrane trafficking and cell signaling), cuticle protein (structural component of insect exoskeleton), and collagen alpha-1 chain (extracellular matrix structure). While these correlations do not imply causation, they suggest potential associations between metabolic changes and gene expression patterns during diapause induction phase. Network analysis revealed stage-specific metabolite-gene correlations during diapause progression. In the DI40 vs. NE comparison, key metabolites included Val-Ser (protein metabolism), sphinganine (membrane structure and signaling), phosphonotyrosine (protein phosphorylation), nandrolone (protein synthesis), and 6-phosphogluconic acid (pentose phosphate pathway), correlating with hornerin expression (epithelial barrier function). The DM20 vs. NE comparison highlighted N-acetylmannosamine (glycoprotein formation), L-cysteine-glutathione disulfide (redox balance), and D-myo-inositol 4-monophosphate (signaling), associated with hornerin, RNA polymerase 2 degradation factor (transcriptional regulation), and collagen alpha-1 chain (extracellular matrix) expression. The recurrence of certain metabolites (e.g., N-acetylmannosamine) and gene types (e.g., collagen and hornerin) across stages suggests their sustained importance throughout diapause.

To elucidate the biochemical and signaling pathways involved in diapause progression of *A. chinensis*, we performed an integrated analysis of differentially expressed genes and differentially abundant metabolites using KEGG pathway mapping (Figures S3G–S3I). DI20 vs. NE comparison group was characterized by significant enrichment in glutathione metabolism, galactose metabolism, and amino sugar and nucleotide sugar metabolism (p < 0.01). DI40 vs. NE comparison group showed sustained importance of amino sugar and nucleotide sugar metabolism, while glutathione metabolism decreased significantly. Notably, sphingolipid metabolism and HIF-1 signaling emerged as significant pathways, potentially reflecting membrane restructuring and hypoxia response activation. DM20 vs. NE comparison group exhibited a distinct shift, with high enrichment in

(B) Volcano plots depicting the differential metabolites in DI20, DI40 and DM20 groups compared to NE group, respectively. Red dots indicate upregulated metabolites, green dots indicate downregulated metabolites, and gray dots represent non-significant changes. The size of dots corresponds to VIP (Variable Importance in Projection) scores.

(C) K-means clustering analysis of metabolite profiles during *A. chinensis* diapause. Heatmap showing the expression patterns of 797 metabolites grouped into eight distinct clusters. The color scale represents Z score normalized abundance levels from −3 (blue) to 4 (red). Different colors in the top bar indicate different diapause stages (NE, DI20, DI40, and DM20), and the left bar shows cluster classification (cluster 1–8).

(D) KEGG pathway annotation of metabolites altered during diapause. Bars represent the number of metabolites associated with each pathway category.

tyrosine metabolism, ferroptosis, and glycine, serine, and threonine metabolism pathways. Interestingly, the estrogen signaling pathway showed increased significance during this phase, hinting at hormonally mediated regulation of diapause maintenance. Notably, the insulin signaling pathway-maintained significance across all stages. The transition from induction to maintenance phases was further marked by increasing importance of various amino acid metabolism pathways (e.g., phenylalanine, alanine, aspartate, and glutamate metabolism) and additional hormone signaling pathways.

DISCUSSION

Glutathione metabolism links ROS level to reflect the redox reaction in *A. chinensis*

Our results revealed a significant downregulation of GSH concentration and GSH/GSSG ratios during the induction and maintenance of diapause in *A. chinensis* (Figure 4). Glutathione, a major intracellular sulfhydryl compound, exists in both reduced (GSH) and oxidized (GSSG) forms. The GSH/GSSG ratio dynamically indicates cellular oxidative stress, with a high ratio suggesting a reduced state and a low ratio indicating an oxidized state.[34] The mitochondrial GSH has been proven to be a crucial factor in controlling mitochondrial metabolic homeostasis, sensing changes in metabolites and facilitating biosynthesis.[35] The content of GSH and GSH/GSSG ratios in *Bombyx mori* during diapause were also decreased, which is similar with our findings.[36] GSH is also a key component of the ROS (Reactive oxygen species) signaling pathway.[37] The levels and oxidation status of GSH are directly regulated by ROS, a class of chemically reactive oxygen metabolites which includes hydroxyl ions, peroxide ions, superoxide anions, singlet-linear oxygen, hypochlorous acid, etc. ROS plays an important role in cell development, growth, metabolism, and defense.[38] The continuous downregulation of GSH and GSH/GSSG ratios during diapause may indicate an increase in ROS levels in *A. chinensis*. ROS has been shown to regulate cyclic arousal during diapause of *Sarcophaga crassipalpis*. This might facilitate the organism switching its main energy metabolism from aerobic to anaerobic in the process of diapause.[8] In addition, ROS can downregulate TCA activity and modulates energy metabolism through the HIF/miR-34/ACS-PK pathway, thereby extending the lifespan of the *Helicoverpa armigera*.[39] ''Oxidoreductase activity'' (GO database) and ''oxidative phosphorylation'' (KEGG database) were significantly enriched in all three comparison groups. Genes associated with these functions were predominantly downregulated during diapause stages compared to non-diapause stage (NE). Thus, we hypothesize that *A. chinensis* adopts a metabolic mode like *Drosophila* during the induction, initiation and maintenance of diapause. Anaerobic glycolysis serves as the primary metabolic mode during the transition to the metabolic inhibition state. However, during the periodic awakening process, aerobic respiration is still performed to maintain protein homeostasis and remove the anaerobic by-products accumulated during the metabolic inhibition state.[8]

Co-expression analysis of the three comparison groups revealed significant upregulation of 5-oxoproline, glycine, and L-pyroglutamic acid in the glutathione metabolic pathway (Table 1). Screening the top 10 positively and negatively expressed genes with the highest correlation coefficients for each metabolite revealed a significant association of cuticle protein with 5-oxoproline, glycine, and L-pyroglutamic acid (Figures 4A–4C). Titin and epidermal proteins are used to build the cuticle, which is the exoskeleton (epidermis) of insects. The cuticle's physical characteristics vary depending on the bodily area and developmental stage, primarily determined by its protein composition.[40] Researchers have discovered that an increase in cuticle proteins during the initial larval development stages, identified through proteomic analysis of different diapause stages in *Culex pipiens*,[41] may enhance epidermal resistance. Furthermore, transcriptome and proteomic approaches were employed by researchers to identify significant correlations of cuticular proteins in adaptation to low-temperature adversity circumstances in studies of cold tolerance in *Solenopsis invicta* and *Cucujus clavipes*.[42,43] We propose that cuticular proteins may contribute to cold tolerance through several mechanisms: (1) Altering the cuticle's physical properties, potentially enhancing epidermal resistance.[40] (2) Interacting with the glutathione metabolite pathway, which is known to play a role in stress response. However, the direct causal relationship between cuticular proteins and cold tolerance requires further investigation. Their upregulation could be part of a broader physiological response to diapause. Future functional studies are needed to elucidate the specific role of cuticular proteins in diapause-related cold tolerance in *A. chinensis* and to explore their potential interactions with other molecular pathways.

Insulin signaling pathway and hormone regulation play crucial roles in regulating diapause of *A. chinensis*

Environmental cues are translated into endogenous hormonal signals, orchestrating a cascade of phenotypic changes in insects. Our transcriptome analysis revealed significant changes in both insulin signaling and juvenile hormone (JH) pathways during diapause. The expression patterns of key JH-related genes suggest a coordinated regulation of JH titers during diapause initiation and maintenance. JHAMT, a critical enzyme in JH biosynthesis,[44] showed continuously decreased expression from NE to DM20, indicating suppressed JH synthesis throughout diapause. Concurrently, JH degradation enzymes (JHEH and JHE-like) exhibited elevated expression during early diapause induction (DI20) followed by a decline, suggesting enhanced JH clearance during diapause initiation. This pattern of reduced JH synthesis coupled with increased degradation likely contributes to the rapid decline in JH titers necessary for diapause induction, similar to observations in other diapausing insects such *Colaphellus bowringi*.[24]

Several studies have indicated the involvement of the insulin signaling pathway in regulating various decelerated characteristics in insects, such as reproductive arrest, extended lifespan, metabolic slowdown, fat accumulation, and enhanced stress tolerance.[25,45,46] Upstream insulin or other growth factors, including phosphatidylinositol 3′-kinase (*PI3K*) and serine/threonine kinase (*Akt*), act as crucial mediators in the signaling pathway, thereby activating various downstream responses.[47]

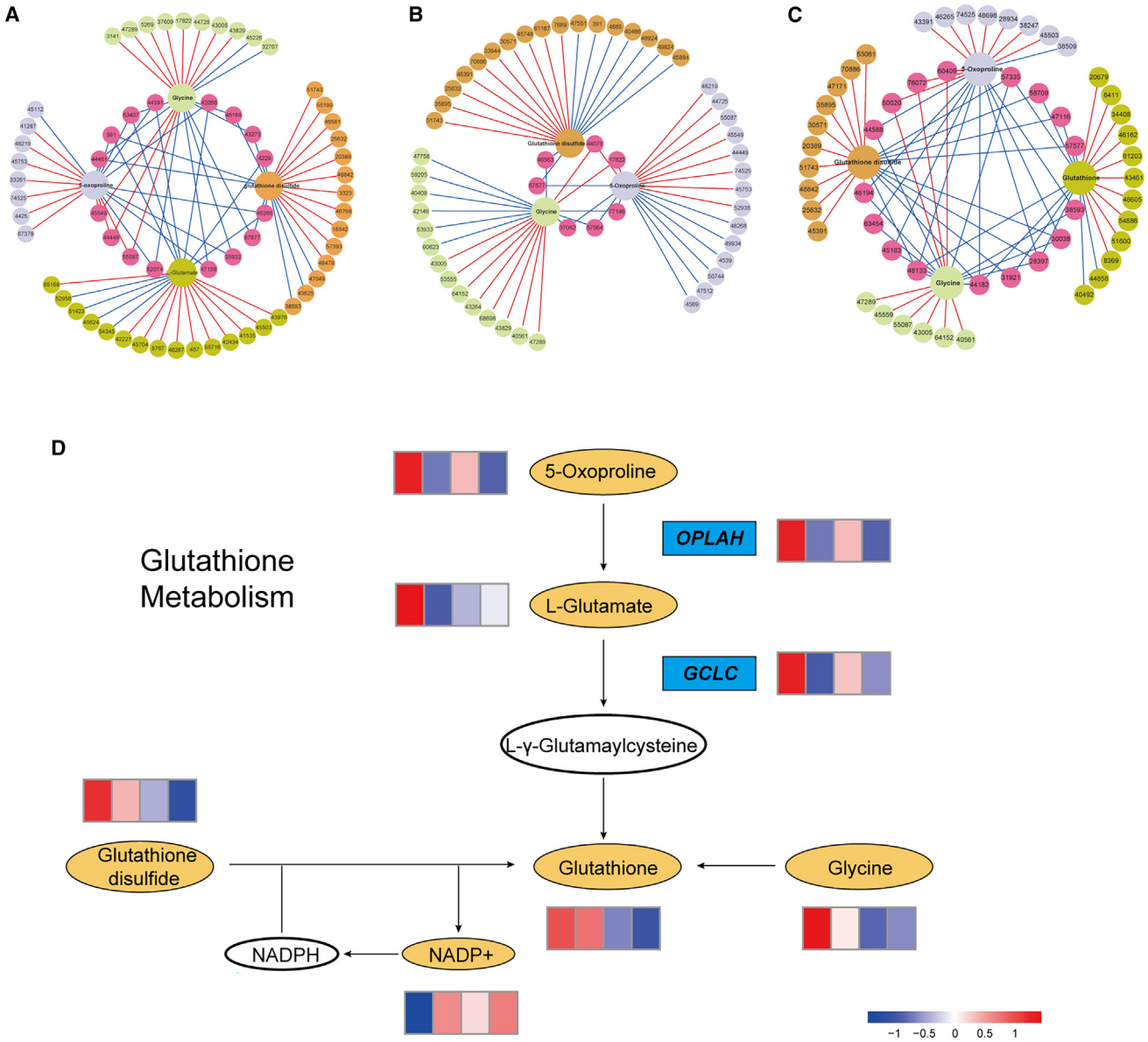

Figure 4. Integrated analysis of differentially expressed genes and differential metabolites involved in glutathione metabolism during diapause of *Arma chinensis*

(A–C) At the stage of DI20 (A), DI40 (B) and DM20 (C). Correlation analysis of genes and metabolites specifically expressed in DI20 (A), DI40 (B) and DM20(C) that are involved in the glutathione pathway. Large circles in the inner layer represent metabolites, and small circles represent genes. Red lines indicate a positive correlation between metabolites and genes, and blue lines indicate a negative correlation. Different metabolites and response genes are represented by the colors green, yellow, purple, and orange, respectively. The pink circle in the center indicates genes that are co-expressed with various metabolites.

(D) Changes in the levels of genes and metabolites involved in the glutathione metabolism pathway. The rectangle was divided into four equal parts (from left to right were NE, DI20, DI40, and DM20). The value was according to the FPKM and intensity value (red indicates upregulation; blue indicates downregulation). OPLAH: 5-oxoprolinase, GCLC: glutamate-cysteine ligase.

Akt phosphorylates and mediates changes in key metabolic targets, regulating forkhead box, class O (*FOXO*) transcription factors involved in cell-cycle arrest, quiescence, lifespan extension, and apoptosis in different systems.[48,49] In our study, *Akt* expression in *A. chinensis* was highest at DI20 and continuously decreased until DM20, implying that *Akt*, a key signaling mediator, exhibits the strongest expression activity during the first 20 days of diapause induction. This change in *Akt* expression appears to regulate several downstream mediators involved in fatty acid biosynthesis and the TCA cycle, potentially inhibiting *FOXO*. Similarly, the inhibition of *Akt* expression can significantly suppress reproductive development and extend lifespan in *Harpegnathos venator*.[50] In *Coccinella septempunctata*, a shutdown of insulin signaling promotes activation of the downstream gene

Table 1. Differential metabolites were identified in DI20, DI40, and DM20 group

Compound Name	Class	DI20vsNE log2FC	DI40vsNE log2FC	DM20vsNE log2FC
N-Acetylmannosamine	Amino acid and its derivatives	−1.4858 ***	−1.6456 ***	−2.11842 ***
2,6-Diaminooimelic Acid	Amino acid and its derivatives	−0.81035 ***	−1.22381 ***	−0.75563 **
5-oxoproline	Amino acid and its derivatives	−0.96661 ***	−1.21997 **	−0.82848 **
Phosphonotyrosine	Amino acid and its derivatives	−0.88713 **	−1.73481 ***	−1.29428 ***
Glycine	Amino acid and its derivatives	−0.52088 **	−0.88692 **	−0.81081 ***
S-adenosyl-L-methioninamine	Amino acid and its derivatives	−1.45709 **	−1.92134 **	−1.61651 **
gamma-Glutamylglutamic acid	Amino acid and its derivatives	−0.64784 **	−1.10695 **	−0.94905 **
4-Hydroxybenzoic acid	Benzoic acid and its derivatives	−1.15861 **	−2.11243 ***	−1.65568 **
D-Myo-inositol 4-monophosohate	Alcohols and polyols	−0.82425 **	−1.61637 ***	−1.39053 ***
1,3-diphopshateglycerate	Glycerolipids	1.725648 **	1.576824 **	1.408739 **
LysoPE 18:2	Phospholipid	1.03719 ***	1.515239 ***	1.474496 ***
PAF C-16	Phospholipid	−1.22288 **	−2.34006 ***	−2.06253 **
alpha-D-Glucose	Carbohydrates and its derivatives	−1.23977 **	−1.56312 **	−1.0821 **
D-Glucopyranose	Carbohydrates and its derivatives	−0.96853 **	−1.19271 **	−0.68502 *
L-Pyroglutamic acid	Organic acid and its derivatives	−0.92422 ***	−1.13712 **	−0.76501 **
Maleic Acid	Organic acid and its derivatives	0.462986 **	0.501681 **	0.661425 ***
2-Oxoadipic acid	Organic acid and its derivatives	0.843846 **	2.237356 ***	1.357675 ***
2-Aminoethylphosphonate	Organic acid and its derivatives	−1.04611 **	−1.0357 **	−1.54973 ***

In the comparison groups DI20vsNE, DI40vsNE, and DM20vsNE, co-expression of distinct metabolites is indicated by asterisks: *$p < 0.05$, **$p < 0.01$, ***$p < 0.001$.

FOXO, leading to the diapause phenotype,[29] which is consistent with our results.

The coordination between insulin signaling and JH pathways appears to be crucial for diapause regulation. While insulin signaling through *Akt* modulates metabolic processes and FOXO-mediated responses, the concurrent suppression of JH signaling ensures reproductive arrest and metabolic adaptation. This hormonal interplay has been documented in other insects, such as *Culex pipiens*,[51] where both insulin and JH signaling are downregulated during diapause.

Phosphoenol pyruvate carboxykinase (*PEPCK*) is a key metabolic enzyme involved in gluconeogenesis, converting oxaloacetate to phosphoenol pyruvate. Several transcriptome studies have identified *PEPCK* as a potentially important factor during diapause and other stress responses.[9,51,52] In *A. chinensis*, we observed that *pepck* expression peaked at DI40 (Figure S2B). While previous studies in *Aedes albopictus* suggested a potential signaling role for *PEPCK* in diapause entry,[53] our findings in *A. chinensis* likely reflect a different function. The upregulation of PEPCK at 40 days of diapause induction is more likely related to its metabolic role, specifically: (1) providing glucose for anaerobic respiration during the hypometabolic state of diapause. (2) Contributing to the synthesis of cryoprotectants, which are crucial for surviving low temperatures during diapause. This interpretation aligns with *PEPCK*'s well-established role in glucose metabolism and its upregulation in various insects during diapause and other stress responses. Further research is needed to fully elucidate the specific metabolic pathways and products associated with *PEPCK* upregulation in diapausing *A. chinensis*.

Energy metabolisms contribute to enhanced survival and cold tolerance of diapausing *A. chinensis*

Insects undergo a resource preparation phase during diapause induction, accumulating diverse energy substances to sustain their vital needs throughout the extended diapause maintenance phase. Both the mosquito *Culex pipiens* and the dark-veined pink butterfly *Pieris napi* undergo lipid accumulation to secure a future energy supply during the overwintering diapause preparation process.[54,55] During diapause induction and maintenance, insects experience significant physiological changes and primarily rely on lipid reserves as their main energy source.[56] However, the metabolism of other nutrients, including amino acids and carbohydrates, also plays important roles in diapause survival and stress tolerance.[57,58]

In our experiment, we found that *A. chinensis* could feed on pupa of the Chinese oak silkworm *Antheraea pernyi* to gain nutrients and energy during the diapause induction phase. Metabolomic analysis revealed that *A. pernyi* pupae contain unsaturated fatty acids (palmitoleic acid, oleic acid, and linolenic acid), amino acids (alanine, proline, and lysine), and rich levels of protein and lipids.[59] Lysosomes function as the digestive system of the cell, serving both to digest macromolecules, old cell parts, and microorganisms in eukaryotic cells. They play important roles in cellular homeostasis, development, and aging. Changes in lysosome function are essential to support cellular adaptation to multiple signals and stimuli.[60] Lysosomes were significantly enriched in both the DI20 vs. NE and DI40 vs. NE comparison groups, as indicated by the KEGG database annotation. This suggests that a significant amount of digestion and energy absorption occurs after *A. chinensis* feed on silkworm pupa at this stage. During the

glycolytic stage of food decomposition, proteins are degraded into amino acids, monosaccharides, and glycogen into glucose, while lipids are converted into smaller molecules following the breakdown of various hydrolytic enzymes.[61] Subsequently, it enters the tricarboxylic acid (TCA) cycle, and the final stage involves energy-producing mechanisms, such as oxidative phosphorylation and electron transport. The alterations in energy metabolism during the induction and maintenance stages of *A. chinensis* are described in the further text from an energy metabolism perspective. Our findings illustrate the participation of numerous metabolites and genes in the energy metabolism pathway.

TCA cycle and glycolysis

During reproductive diapause of *A. chinensis*, we observed significant changes in energy metabolism pathways, particularly in glycolysis and the TCA cycle. Similarly, the TCA cycle undergoes significant changes during diapause induction of the East Asian locust *Locusta migratoria*.[62] The flesh fly *S. crassipalpis* pupae exhibit alternating metabolic inhibition and periodic arousal during different diapause periods, attributed to varying dominance of glycolysis and the TCA cycle.[8] Our results also support the hypothesis proposed for *H. armigera*, suggesting that the brain controls the TCA cycle to reduce metabolic intensity and manage lipid accumulation in the fat body.[63] This mechanism may be conserved across different insect species, including *A. chinensis*. The dynamic alterations we observed in the TCA cycle, glycolysis, and other energy metabolic processes in *A. chinensis* during diapause underscore the crucial role of energy metabolism in controlling the diapause process. These changes likely contribute to the insect's ability to survive extended periods of unfavorable conditions while maintaining the capacity for post-diapause development.

In the glycolytic pathway, a primary energy metabolic route in insects, glucose is catabolized to produce pyruvate. Our metabolite measurements at different diapause stages showed continuous decreases in glucose, glucose 1-phosphate, and glucose 6-phosphate from NE to DI40, with no significant change from DI40 to DM20. Pyruvate levels showed a more complex pattern, decreasing from NE to DI20, increasing from DI20 to DI40, and decreasing again from DI40 to DM20. The observed decrease in glucose and its phosphorylated forms during diapause induction in *A. chinensis* suggests an active utilization of these metabolites. This could be attributed to several possible mechanisms: (1) enhanced glycolysis to meet immediate energy demands during the transition to diapause. (2) Conversion of glucose to glycerol or other polyols, which are known cryoprotectants in many insects. (3) Utilization in other metabolic pathways that becomes more active during diapause initiation. The fluctuation in pyruvate levels might reflect a balance between its production through glycolysis and its consumption in various metabolic processes, including potential conversion to lactate under low-oxygen conditions or entry into the TCA cycle. These metabolic changes likely represent part of *A. chinensis*' physiological preparation for diapause, potentially contributing to cold tolerance. However, the specific roles of these metabolites in cold resistance require further investigation.

In the glycolytic pathway, a primary energy metabolic route in insects, glucose is catabolized to produce pyruvate. Our metabolite measurements at different diapause stages revealed complex changes in key metabolites. Glucose, glucose 1-phosphate, and glucose 6-phosphate continuously decreased from NE to DI40, with no significant change from DI40 to DM20. Pyruvate showed a more dynamic pattern: decreasing from NE to DI20, increasing from DI20 to DI40, and decreasing again from DI40 to DM20. These changes suggest active metabolic regulation during diapause induction and maintenance in *A. chinensis*. The decrease in glucose and its phosphorylated forms could indicate enhanced glycolysis to meet immediate energy demands during the transition to diapause. Alternatively, it might suggest the conversion of glucose to cryoprotectants, such as glycerol, sorbitol, or erythritol. The fluctuation in pyruvate levels might reflect a balance between its production through glycolysis and its consumption in various metabolic processes. The increase in pyruvate from DI20 to DI40 is, particularly interesting. During the maintenance stage (DM20), we observed stable glucose levels but decreased pyruvate content. This is contrary to the findings in *Helicoverpa armigera*, where increased pyruvate levels were associated with metabolic slowdown during diapause.[64] The difference suggests that pyruvate metabolism during diapause may vary among insect species. The complex changes in glucose and pyruvate metabolism during diapause of *A. chinensis* likely contribute to both energy regulation and cold tolerance. However, the specific mechanisms require further investigation. Future studies should focus on quantifying changes in known cryoprotectants to directly link glucose depletion with cold tolerance. Additionally, exploring species-specific differences in pyruvate metabolism during diapause and investigating the enzymatic activities in glycolysis and related pathways will enhance our understanding of the metabolic flux during diapause.

Our data showed that after 40 days of diapause induction, *A. chinensis* entered a hypometabolic state in which the expressions of hexokinase (*HK*) and pyruvate kinase (*PK*) were lowest at DI40 and their expression at DI20 and DM20 was higher than that at DI40, respectively. This was consistent with the expression trend of metabolites in the glycolysis stage and jointly regulated the metabolic process. These key genes such as *HK* and *PK* involved in the glycolytic pathway play crucial roles in metabolic regulation and stress resistance in many insect species. For instance, the reduction of *HK* expression induces diapause and prolongs the lifespan of *H. armigera* larvae, and *HK* also acts as a crucial regulator of energy metabolism and ROS activity during the extended diapause period.[65] Similarly, *Eurosta solidaginis* can reduce its metabolic rate and accumulate the cryoprotective chemical polyol cryoprotectant as a response to cold stimuli.[66]

Our metabolomic analysis revealed changes in tricarboxylic acid (TCA) cycle intermediates during *A. chinensis* diapause. Intermediate products of the TCA cycle (such as oxaloacetate, α-ketoglutarate) serve as raw materials for synthesizing sugars, amino acids, and fats. For instance, oxaloacetate can decarboxylate into phosphoenolpyruvate, participating in fatty acid synthesis. The TCA cycle serves as a hub linking the metabolism of the three major substances, sugars, amino acids, and fats, and energy metabolism. To adapt to low temperatures, *Cinara tujafilina* inactivates the glycolytic pathway and the TCA cycle.[67] When the *Sitodiplosis mosellana* enters diapause, its metabolic activity is inhibited, as indicated by a decrease in the levels of

malic acid, citric acid, ferredoxin, and α-ketoglutaric acid.[14] During the 20-day diapause induction period under low temperature and short photoperiod conditions, we identified six metabolites involved in the TCA cycle: oxaloacetate, citric acid, α-ketoglutaric acid, succinic acid, ferredoxin, and malic acid. While some metabolites like oxaloacetate, α-ketoglutarate, ferredoxin, and malic acid showed no significant changes after entering diapause, others exhibited a dynamic pattern. The expression of key TCA cycle enzymes, including fumarate hydratase (fum), Succinate dehydrogenase (*SDHA*), ATP citrate(pro-S)-lyase (*ACLY*), aconitate hydratase (*ACO*), and succinyl-CoA synthetase alpha subunit (*sucD*), followed a similar trend: decreasing from NE to DI20, increasing to DI40, and decreasing again to DM20 (Figure S2C). These changes suggest a shift in energy metabolism during diapause induction. Within the first 20 days, *A. chinensis* likely increased metabolic intensity to resist cold stimuli, primarily consuming energy substances. Between 20 and 40, a metabolic switch from aerobic to stored energy utilization seems to have occurred. During the subsequent maintenance phase, metabolism appeared to shift to a low-energy state dominated by anaerobic processes. However, it's important to note that these interpretations are based on steady-state metabolite levels and gene expression, which don't directly measure metabolic flux. Future studies using metabolic flux analysis could provide more definitive insights into TCA cycle dynamics during *A. chinensis* diapause.

Lipid metabolism

Insects rely on lipids for energy storage and as structural components of the epidermis and cell membranes. They possess a metabolic pathway that facilitates the conversion of glucose into lipids, with many insects capable of synthesizing and storing lipids in their fat bodies. Sterols are crucial for insect survival, making them a necessary component of all insect diets. Additionally, insects, like many others, necessitate a diet rich in polyunsaturated fatty acids (PUFAs), such as palmitoleic acid and linoleic acid. Using GC/MS techniques, researchers analyzed the lipid content of overwintering nymphs of *Megachile rotundata*, an alfalfa leaf-cutting bee. Research revealed that triglycerides constituted over 80% of the nymphs' lipids, with palmitoleic and linolenic acids being the predominant components within the triglycerides.[68] Our results revealed that during diapause induction, *A. chinensis* exhibited similar expression patterns for palmitoleic acid and linoleic acid: both were downregulated from NE to DI20, upregulated at DI40, and downregulated at DM20, with the highest concentration observed at DI40. Fatty acid regulation begins with acetyl-CoA carboxylase (ACC), followed by conversion from acetyl-CoA to malonyl-CoA by fatty acid synthase (FAS); thus, any changes in these enzymes produce the same outcome.[69,70] In the diapause phase of *C. septempunctata*, lipid accumulation was dependent on *ACC*,[71] and *FAS* is associated with lipid accumulation and cold tolerance during diapause induction of *Colaphellus bowringi*.[24] Similarly, our data demonstrated that the highest expression levels of both *ACC* and *FAS* were noted at DI40. The triglyceride content in *A. chinensis* fluctuates during diapause, initially decreasing slightly at DI20, then peaking at DI40, before decreasing again at DM20 to levels like those observed in diapause induction stage. These findings support the conclusions (Figures S2A and S2B).

Dihydroxyacetone phosphate and citric acid, key intermediates in glycolysis and the TCA cycle, respectively, are important for energy metabolism and fatty acid synthesis. The contents of both metabolites decreased from NE to DI40, with dihydroxyacetone phosphate continuing to decrease during DM20 while citric acid increased. These changes suggest dynamic shifts in lipid metabolism during *A. chinensis* diapause. The initial decrease might indicate increased lipid utilization, particularly triglycerides, during diapause induction. The subsequent upregulation of lipid synthesis-related metabolites and genes from DI20 to DI40 could reflect energy storage preparation for diapause.

Carbohydrate metabolism

Sugars are essential components of almost all insect diets due to their vital role as a source of energy and their capacity to be converted into lipids and amino acids. Previous research indicates that trehalose provides energy to insects and is being investigated as a potential cryoprotectant. *S. mosellana* exhibited significantly increased trehalose levels during both diapause induction and maintenance, compared to non-diapause insects.[14] *A. pernyi*'s diapause release pathway is regulated by 20-hydroxyecdysone and controlled by trehalose metabolism during diapause.[72] Our findings reveal continuous trehalose accumulation during *A. chinensis*' diapause induction, reaching its peak at DI40 and decreasing until DM20. Additionally, trehalase was continuously downregulated during diapause induction and upregulated from DI40 to DM20. We hypothesize that trehalose acts as a cryoprotectant during *A. chinensis*' diapause phase. Similarly, *Sericinus montelus* showed significantly upregulated trehalose concentration during diapause, suggesting its role as a major cryoprotectant for overwintering nymphs, increasing their cold tolerance ability.[73] Cryoprotection against cold stress in *S. mosellana* primarily involves the use of trehalose.[19]

Sorbitol is a prevalent component in various insects and serves as their primary energy source in metabolism, including species like the cotton bollworm and the silkworm. Sorbitol plays a crucial role during diapause as it provides essential energy to sustain the organism, enabling insects to endure the diapause and continue their life cycle successfully.[74] In *Ostrinia nubilalis* diapause, sorbitol content is notably reduced in response to lowered temperatures.[75] Additionally, our findings demonstrated that *A. chinensis* accumulated sorbitol from NE to DI20, followed by a downregulation until DI40, with no significant changes observed until the DM20 stage. A previous study on the linden bug *Pyrrhocoris apterus* revealed that it accumulated sorbitol in response to low-temperature triggers during the adult diapause phase.[11] Our results align with those of *P. apterus*, providing evidence that diapause and cold hardiness may be coincidental.

We hypothesize that *A. chinensis* accumulates trehalose and sorbitol during the diapause induction period to provide the energy required for cold tolerance. During the diapause maintenance phase, trehalose content significantly decreased, while sorbitol exhibited no significant changes. These findings suggest that the two metabolites may serve different functions at different diapause stages. In conclusion, carbohydrates play a crucial role in providing energy during *A. chinensis*' diapause; however, additional data are required to identify specific sugars that are vital for energy supply at different diapause phases. Additionally,

measuring the body's supercooling point (SCP) can help assess the cold hardiness ability of *A. chinensis*.

Amino acid metabolism

Amino acids play a crucial role as essential nutrients in protein synthesis, particularly during biological growth stages and neurotransmission. *Drosophila* requires 10 essential amino acids for proper function, and females particularly depend on amino acid-rich food to meet their egg-laying requirements.[76] Enhanced cold resistance in lagomorphic insects exposed to cold diapause induction results from specific characteristics, such as metabolic inhibition and the production of cryoprotective chemicals.[77] The category of amino acids and their derivatives exhibited the highest number of metabolites in each comparison group, and the metabolic pathways associated with amino acids showed significant enrichment with diverse metabolites, as indicated by the data. Metabolic pathways involving valine, leucine, and isoleucine degradation, tyrosine metabolism, lysine synthesis, and glycine, serine, and threonine metabolism were all significantly enriched in the three comparison groups, suggesting that these pathways played a prominent role in amino acid metabolism during the diapause process.

Insects can utilize various amino acids, including serine, glycine, and threonine, for pyruvate production. Pyruvate serves as a vital intermediate in the glycolytic metabolism of all living cells and facilitates the interconversion of various chemicals *in vivo*.[78,79] This suggests that the increase in pyruvate during diapause might be associated with a decline in certain chemicals. Previous studies have reported reduced levels of glycine and serine in the adults of the mite *Tetranychus urticae* and the European corn borer *Ostrinia nubilalis* during diapause.[17,80] Our findings align with this pattern, as we observed a similar trend in glycine and serine levels throughout *A. chinensis* diapause, with a downregulation during diapause induction and an upregulation during diapause maintenance. Research on the *S. crassipalpis*, a member of the Sparidae family, revealed significant accumulation of glutamine. Additionally, it was found that glutamine significantly enhanced the cold tolerance of the diapausing insects.[81] Our study revealed that glutamine was downregulated during the 20-day stage of diapause induction but showed continuous upregulation from DI20 to DM20, potentially enhancing the diapausing insects' ability to endure low temperatures during diapause induction after 20 days.

Glutamate serves as a crucial neurotransmitter in the animal nervous system, playing a pivotal role from invertebrates to mammals.[82] Studies on insects have revealed a considerable presence of glutamatergic neurons in the central nervous system.[83,84] Additionally, glutamatergic transmission plays a role in various physiological processes in insects, encompassing sleep, circadian movement, and reproduction.[85–87] A study on the stunted reproduction of *Riptortus pedestris*, a member of the Rimantidae family of point marmorated stink bugs, indicated that glutamate might participate in the transfer of photoperiodic signals from biological clock cells to reproductive control cells, thereby regulating the stunted reproduction of the point marmorated stink bug.[32] In the *A. chinensis*, glutamate exhibited a significant downregulation from first eclosion to 20 days of diapause induction, as indicated by the metabolomic data. Following this, there was a continuous upregulation trend until 20 days of diapause maintenance. The findings suggest that glutamate might significantly respond to photoperiod and temperature changes during the early stage of diapause induction, leading to downregulation of glutamate content. Subsequently, after DI20, the *A. chinensis* gradually adapted to cold environmental conditions, leading to a gradual upregulation of glutamate content.

In conclusion, diapause in *A. chinensis* involves specific changes in amino acid-related metabolites and genes, likely associated with energy supply and defense against damage from cold environmental stimuli.

Conclusions

Our results presented in this study validate our initial hypotheses regarding metabolic regulation during *A. chinensis* diapause. Supporting our hypothesis of significant metabolic reprogramming, transcriptome analysis revealed thousands of DEGs during diapause induction and maintenance, with key regulatory genes such as *DR-2*, *JHAMT*, and *PK* showing consistent expression patterns between RNA-seq and RT-qPCR validation.

The metabolomics analysis confirmed our hypothesis of distinct metabolic strategies between pre-diapause and diapause maintenance phases by revealing phase-specific metabolic signatures. We observed dynamic changes in energy-related pathways, including glycolysis, TCA cycle, and carbohydrate metabolism. During diapause maintenance, we observed accumulation of cryoprotectants (trehalose and sorbitol) and energy storage compounds (triglycerides), indicating adaptive metabolic adjustments.

Our analysis also supported the hypothesis regarding crucial pathway-specific roles in facilitating diapause. The glutathione metabolism pathway emerged as essential in redox regulation, while the insulin signaling pathway, particularly through *Akt* and *PEPCK*, appeared to regulate diapause-associated processes. Additionally, amino acid metabolism pathways showed significant alterations in glycine, serine, glutamine, and glutamate levels.

These findings provide strong support for our hypotheses and offer a comprehensive understanding of the stage-specific metabolic adjustments during *A. chinensis* diapause. This knowledge may contribute to improving biocontrol agent production and storage strategies.

Limitations of the study

Although this study provides comprehensive insights into the metabolic regulation of diapause in *A. chinensis*, several limitations should be noted. Our analyses provide correlative evidence for metabolic changes during diapause, but causal relationships require further functional validation through genetic approaches. The study focused exclusively on female adults, leaving sex-specific differences in diapause regulation unexplored. While our metabolomic and transcriptomic analyses revealed significant pathway changes, steady-state measurements may not fully capture the dynamic nature of metabolic flux. Additionally, the temporal resolution of our sampling strategy may have missed rapid metabolic transitions between the examined time points. Future studies employing more frequent sampling, metabolic flux analysis, and investigation of sex-specific differences

would address these limitations and further advance our understanding of diapause regulation.

RESOURCE AVAILABILITY

Lead contact

Further information and requests for resources and reagents should be directed to and will be fulfilled by the lead contact, Lisheng Zhang (zhangleesheng@163.com).

Materials availability

All unique reagents generated in this study are available from the lead contact with a completed Materials Transfer Agreement.

Data and code availability

- Data supporting the findings in this study are included in the article and Supplementary Tables and Figures.
- The raw RNA-seq data generated in this study have been deposited in the National Center for Biotechnology Information (NCBI) Sequence Read Archive (SRA) database under accession number PRJNA1154624. These data can be accessed through rocid using the credentials provided upon request.
- The metabolomics data have been deposited in the MetaboLights database under accession number MTBLS11731.
- Further inquiries can be directed to the corresponding authors.

ACKNOWLEDGMENTS

This research was funded by National Key R&D Program of China (2021YFD1400703, 2023YFE0123000), the Major Project of China National Tobacco Corporation (110202201022 (LS-06)) and Guizhou Provincial Tobacco Corporation Project (2024XM07).

AUTHOR CONTRIBUTIONS

M.Z.: conceptualization, data curation, formal analysis, investigation, methodology, resources, visualization, writing—review and editing. W.H.: formal analysis, writing—review and editing. Y.L.: writing—review and editing, writing—original draft. J.C. and N.M.T.: writing—review and editing. L.Z.: funding acquisition, investigation, project administration, writing—review and editing.

DECLARATION OF INTERESTS

The authors declare that they have no conflicts of interest.

STAR★METHODS

Detailed methods are provided in the online version of this paper and include the following:

- KEY RESOURCES TABLE
- EXPERIMENTAL MODEL AND STUDY PARTICIPANT DETAILS
- METHOD DETAILS
  - Insect rearing and micrographic examination
  - Transcriptome sequencing and data analysis
  - Metabolite profiling analysis
  - qRT-PCR verification of RNA-Seq
  - Triglyceride measurement
  - Integrated analysis of transcriptomics and metabolomics
- QUANTIFICATION AND STATISTICAL ANALYSIS
- ADDITIONAL RESOURCES

SUPPLEMENTAL INFORMATION

Supplemental information can be found online at https://doi.org/10.1016/j.isci.2025.111761.

Received: September 19, 2024
Revised: November 5, 2024
Accepted: January 3, 2025
Published: January 6, 2025

REFERENCES

1. Numata, H., and Shintani, Y. (2023). Diapause in Univoltine and Semivoltine Life Cycles. Annu. Rev. Entomol. *68*, 257–276. https://doi.org/10.1146/annurev-ento-120220-101047.
2. Denlinger, D.L. (2023). Insect diapause: from a rich history to an exciting future. J. Exp. Biol. *226*, jeb245329. https://doi.org/10.1242/jeb.245329.
3. Kostál, V. (2006). Eco-physiological phases of insect diapause. J. Insect Physiol. *52*, 113–127. https://doi.org/10.1016/j.jinsphys.2005.09.008.
4. Torson, A.S., Bowman, S., Doucet, D., Roe, A.D., and Sinclair, B.J. (2023). Molecular signatures of diapause in the Asian longhorned beetle: Gene expression. Curr. Res. Insect Sci. *3*, 100054. https://doi.org/10.1016/j.cris.2023.100054.
5. Karp, X. (2021). Hormonal regulation of diapause and development in nematodes, insects, and fishes. Front. Ecol. Evol. *9*, 735924. https://doi.org/10.1073/pnas.1804590115.
6. Denlinger, D.L. (2008). Why study diapause? Entomol. Res. *38*, 1–9. https://doi.org/10.1111/j.1748-5967.2008.00139.x.
7. Denlinger, D.L. (2022). Insect Diapause. Am. Entomol. *68*, 61–62. https://doi.org/10.1093/ae/tmac047.
8. Chen, C., Mahar, R., Merritt, M.E., Denlinger, D.L., and Hahn, D.A. (2021). ROS and hypoxia signaling regulate periodic metabolic arousal during insect dormancy to coordinate glucose, amino acid, and lipid metabolism. Proc. Natl. Acad. Sci. USA *118*, e2017603118. https://doi.org/10.1073/pnas.2017603118.
9. Wang, T., Geng, S.L., Guan, Y.M., and Xu, W.H. (2018). Deacetylation of metabolic enzymes by Sirt2 modulates pyruvate homeostasis to extend insect lifespan. Aging (Albany NY) *10*, 1053–1072. https://doi.org/10.18632/aging.101447.
10. Ramírez-Soria, M.J., Wäckers, F., and Sanchez, J.A. (2019). When natural enemies go to sleep: diapause induction and termination in the pear psyllid predator *Pilophorus gallicus* (Hemiptera: Miridae). Pest Manag. Sci. *75*, 3293–3301. https://doi.org/10.1002/ps.5451.
11. Koštál, V., Tamura, M., Tollarová, M., and Zahradníčková, H. (2004). Enzymatic capacity for accumulation of polyol cryoprotectants changes during diapause development in the adult red firebug, *Pyrrhocoris apterus*. Physiol. Entomol. *29*, 344–355. https://doi.org/10.1111/j.0307-6962.2004.00396.x.
12. Hahn, D.A., and Denlinger, D.L. (2011). Energetics of insect diapause. Annu. Rev. Entomol. *56*, 103–121. https://doi.org/10.1146/annurev-ento-112408-085436.
13. MacRae, T.H. (2010). Gene expression, metabolic regulation and stress tolerance during diapause. Cell. Mol. Life Sci. *67*, 2405–2424. https://doi.org/10.1007/s00018-010-0311-0.
14. Huang, Q., Ma, Q., Li, F., Zhu-Salzman, K., and Cheng, W. (2022). Metabolomics reveals changes in metabolite profiles among pre-diapause, diapause and post-diapause larvae of *Sitodiplosis mosellana* (Diptera: Cecidomyiidae). Insects *13*, 339. https://doi.org/10.3390/insects13040339.
15. Penkov, S., Raghuraman, B.K., Erkut, C., Oertel, J., Galli, R., Ackerman, E.J.M., Vorkel, D., Verbavatz, J.M., Koch, E., Fahmy, K., et al. (2020). A metabolic switch regulates the transition between growth and diapause in *C. elegans*. BMC Biol. *18*, 31. https://doi.org/10.1186/s12915-020-0760-3.
16. Purać, J., Kojić, D., Popović, Ž.D., Vukašinović, E., Tiziani, S., and Günther, U.L. (2015). Metabolomic analysis of diapausing and non-diapausing larvae of the european corn borer *Ostrinia nubilalis* (Hbn.) (Lepidoptera: Crambidae). Acta Chim. Slov. *62*, 761–767.

17. Khodayari, S., Moharramipour, S., Larvor, V., Hidalgo, K., and Renault, D. (2013). Deciphering the metabolic changes associated with diapause syndrome and cold acclimation in the two-spotted spider mite *Tetranychus urticae*. PLoS One *8*, e54025. https://doi.org/10.1371/journal.pone.0054025.

18. Li, Y., Zhang, L., Chen, H., Koštál, V., Simek, P., Moos, M., and Denlinger, D.L. (2015). Shifts in metabolomic profiles of the parasitoid *Nasonia vitripennis* associated with elevated cold tolerance induced by the parasitoid's diapause, host diapause and host diet augmented with proline. Insect Biochem. Mol. Biol. *63*, 34–46. https://doi.org/10.1016/j.ibmb.2015.05.012.

19. Huang, Q., Zhang, G., Nan, J., Cheng, W., and Zhu-Salzman, K. (2021). Characterization of trehalose metabolic genes and corresponding enzymatic activities during diapause of *Sitodiplosis mosellana*. J. Insect Physiol. *135*, 104324. https://doi.org/10.1016/j.jinsphys.2021.104324.

20. Goto, M., Li, Y.P., Kayaba, S., Outani, S., and Koichi, S. (2001). Cold hardiness in summer and winter diapause and post-diapause pupae of the cabbage armyworm, *Mamestra brassicae* L. under temperature acclimation. J. Insect Physiol. *47*, 709–714. https://doi.org/10.1016/s0022-1910(00)00164-5.

21. Hahn, D.A., and Denlinger, D.L. (2007). Meeting the energetic demands of insect diapause: nutrient storage and utilization. J. Insect Physiol. *53*, 760–773. https://doi.org/10.1016/j.jinsphys.2007.03.018.

22. Ciancio, J.J., Turnbull, K.F., Gariepy, T.D., and Sinclair, B.J. (2021). Cold tolerance, water balance, energetics, gas exchange, and diapause in overwintering brown marmorated stink bugs. J. Insect Physiol. *128*, 104171. https://doi.org/10.1016/j.jinsphys.2020.104171.

23. Moraes, B., Braz, V., Santos-Araujo, S., Oliveira, I.A., Bomfim, L., Ramos, I., and Gondim, K.C. (2022). Deficiency of acetyl-coA carboxylase impairs digestion, lipid synthesis, and reproduction in the kissing bug *Rhodnius prolixus*. Front. Physiol. *13*, 934667. https://doi.org/10.3389/fphys.2022.934667.

24. Tan, Q.Q., Liu, W., Zhu, F., Lei, C.L., and Wang, X.P. (2017). Fatty acid synthase 2 contributes to diapause preparation in a beetle by regulating lipid accumulation and stress tolerance genes expression. Sci. Rep. *7*, 40509. https://doi.org/10.1038/srep40509.

25. Miki, T., Shinohara, T., Chafino, S., Noji, S., and Tomioka, K. (2020). Photoperiod and temperature separately regulate nymphal development through JH and insulin/TOR signaling pathways in an insect. Proc. Natl. Acad. Sci. USA *117*, 5525–5531. https://doi.org/10.1073/pnas.1922747117.

26. Sim, C., and Denlinger, D.L. (2013). Insulin signaling and the regulation of insect diapause. Front. Physiol. *4*, 189. https://doi.org/10.3389/fphys.2013.00189.

27. Chen, J.J., Liu, X.X., Guo, P.H., Teets, N.M., Zhou, J.C., Chen, W.B., Luo, Q.Z., Kanjana, N., Li, Y.Y., and Zhang, L.S. (2024). Regulation of forkhead box O transcription factor by insulin signaling pathway controls the reproductive diapause of the lady beetle, *Coccinella septempunctata*. Int. J. Biol. Macromol. *258*, 128104. https://doi.org/10.1016/j.ijbiomac.2023.128104.

28. Tang, Y.T., Guo, Y., Pan, M.Z., Mao, J.J., Chen, H.Y., Zhang, L.S., and Wang, M.Q. (2020). Predation of *Plutella xylostella* larva by *Arma chinensis*. Plant Prot. *46*, 155–160.

29. Tang, Y.T., Li, Y.Y., Liu, C.X., Mao, J.J., Chen, H.Y., Zhang, L.S., and Wang, M.Q. (2019). Predation and behavior of *Arma chinensis* to *Spodoptera frugiperda*. Plant Prot. *45*, 65–68.

30. Chen, J., Guo, P., Li, Y., He, W., Chen, W., Shen, Z., Zhang, M., Mao, J., and Zhang, L. (2022). Cathepsin L contributes to reproductive diapause by regulating lipid storage and survival of *Coccinella septempunctata* (Linnaeus). Int. J. Mol. Sci. *24*, 611. https://doi.org/10.3390/ijms24010611.

31. Easwaran, S., Van Ligten, M., Kui, M., and Montell, D.J. (2022). Enhanced germline stem cell longevity in *Drosophila* diapause. Nat. Commun. *13*, 711. https://doi.org/10.1038/s41467-022-28347-z.

32. Hasebe, M., and Shiga, S. (2022). Clock gene-dependent glutamate dynamics in the bean bug brain regulate photoperiodic reproduction. PLoS Biol. *20*, e3001734. https://doi.org/10.1371/journal.pbio.3001734.

33. Pegoraro, M., Fishman, B., Zonato, V., Zouganelis, G., Francis, A., Kyriacou, C.P., and Tauber, E. (2022). Photoperiod-dependent expression of microRNA in *Drosophila*. Int. J. Mol. Sci. *23*, 4935. https://doi.org/10.3390/ijms23094935.

34. Asensi, M., Sastre, J., Pallardo, F.V., Lloret, A., Lehner, M., Garcia-de-la Asuncion, J., and Viña, J. (1999). Ratio of reduced to oxidized glutathione as indicator of oxidative stress status and DNA damage. Methods Enzymol. *299*, 267–276. https://doi.org/10.1016/s0076-6879(99)99026-2.

35. Liu, Y., Liu, S., Tomar, A., Yen, F.S., Unlu, G., Ropek, N., Weber, R.A., Wang, Y., Khan, A., Gad, M., et al. (2023). Autoregulatory control of mitochondrial glutathione homeostasis. Science *382*, 820–828. https://doi.org/10.1126/science.adf4154.

36. Meng, G., Yao, J., Wang, L., and Zhao, L. (2011). Variation in glutathione status associated with induction and initiation of diapause in eggs of the bivoltine strain of the silkworm *Bombyx mori*. Physiol. Entomol. *36*, 173–179. https://doi.org/10.1111/j.1365-3032.2011.00783.x.

37. Chen, S., Lu, M., Zhang, N., Zou, X., Mo, M., and Zheng, S. (2018). Nuclear factor erythroid-derived 2-related factor 2 activates glutathione S-transferase expression in the midgut of *Spodoptera litura* (Lepidoptera: Noctuidae) in response to phytochemicals and insecticides. Insect Mol. Biol. *27*, 522–532. https://doi.org/10.1111/imb.12391.

38. Ghanta, S., and Chattopadhyay, S. (2011). Glutathione as a signaling molecule: another challenge to pathogens. Plant Signal. Behav. *6*, 783–788. https://doi.org/10.4161/psb.6.6.15147.

39. Wang, Z.H., Jiang, S., and Xu, W.H. (2023). ROS downregulate TCA activity to modulate energy metabolism via the HIF/miR-34/ACS-PK pathway for lifespan extension in *Helicoverpa armigera*. Biochim. Biophys. Acta Mol. Cell Res. *1870*, 119414. https://doi.org/10.1016/j.bbamcr.2022.119414.

40. Charles, J.P. (2010). The regulation of expression of insect cuticle protein genes. Insect Biochem. Mol. Biol. *40*, 205–213. https://doi.org/10.1016/j.ibmb.2009.12.005.

41. Li, A., and Denlinger, D.L. (2009). Pupal cuticle protein is abundant during early adult diapause in the mosquito *Culex pipiens*. J. Med. Entomol. *46*, 1382–1386. https://doi.org/10.1603/033.046.0618.

42. Carrasco, M.A., Buechler, S.A., Arnold, R.J., Sformo, T., Barnes, B.M., and Duman, J.G. (2011). Elucidating the biochemical overwintering adaptations of larval *Cucujus clavipes* puniceus, a nonmodel organism, via high throughput proteomics. J. Proteome Res. *10*, 4634–4646. https://doi.org/10.1021/pr200518y.

43. Vatanparast, M., Puckett, R.T., Choi, D.S., and Park, Y. (2021). Comparison of gene expression in the red imported fire ant (*Solenopsis invicta*) under different temperature conditions. Sci. Rep. *11*, 16476. https://doi.org/10.1038/s41598-021-95779-w.

44. Shinoda, T., and Itoyama, K. (2003). Juvenile hormone acid methyltransferase: a key regulatory enzyme for insect metamorphosis. Proc. Natl. Acad. Sci. USA *100*, 11986–11991. https://doi.org/10.1073/pnas.2134232100.

45. Chen, J., Cui, D.N., Ullah, H., Li, S., Pan, F., Xu, C.M., Tu, X.B., and Zhang, Z.H. (2020). The Function of LmPrx6 in Diapause Regulation in *Locusta migratoria* Through the Insulin Signaling Pathway. Insects *11*, 763. https://doi.org/10.3390/insects11110763.

46. Jordan, J.M., Hibshman, J.D., Webster, A.K., Kaplan, R.E.W., Leinroth, A., Guzman, R., Maxwell, C.S., Chitrakar, R., Bowman, E.A., Fry, A.L., et al. (2019). Insulin/IGF signaling and vitellogenin provisioning mediate intergenerational adaptation to nutrient stress. Curr. Biol. *29*, 2380–2388. https://doi.org/10.1016/j.cub.2019.05.062.

47. Manning, B.D., and Toker, A. (2017). AKT/PKB signaling: navigating the network. Cell *169*, 381–405. https://doi.org/10.1016/j.cell.2017.04.001.

48. Aghayeva, U., Bhattacharya, A., Sural, S., Jaeger, E., Churgin, M., Fang-Yen, C., and Hobert, O. (2021). DAF-16/FoxO and DAF-12/VDR control

cellular plasticity both cell-autonomously and via interorgan signaling. PLoS Biol. *19*, e3001204. https://doi.org/10.1371/journal.pbio.3001204.

49. Olademehin, O.P., Liu, C., Rimal, B., Adegboyega, N.F., Chen, F., Sim, C., and Kim, S.J. (2020). Dsi-RNA knockdown of genes regulated by Foxo reduces glycogen and lipid accumulations in diapausing *Culex pipiens*. Sci. Rep. *10*, 17201. https://doi.org/10.1038/s41598-020-74292-6.
50. Yan, H., Opachaloemphan, C., Carmona-Aldana, F., Mancini, G., Mlejnek, J., Descostes, N., Sieriebriennikov, B., Leibholz, A., Zhou, X., Ding, L., et al. (2022). Insulin signaling in the long-lived reproductive caste of ants. Science *377*, 1092–1099. https://doi.org/10.1126/science.abm8767.
51. Sim, C., and Denlinger, D.L. (2008). Insulin signaling and FOXO regulate the overwintering diapause of the mosquito *Culex pipiens*. Proc. Natl. Acad. Sci. USA *105*, 6777–6781. https://doi.org/10.1073/pnas.0802067105.
52. Poelchau, M.F., Reynolds, J.A., Elsik, C.G., Denlinger, D.L., and Armbruster, P.A. (2013). Deep sequencing reveals complex mechanisms of diapause preparation in the invasive mosquito, *Aedes albopictus*. Proc. Biol. Sci. *280*, 20130143. https://doi.org/10.1098/rspb.2013.0143.
53. Poelchau, M.F., Reynolds, J.A., Denlinger, D.L., Elsik, C.G., and Armbruster, P.A. (2011). A *de novo* transcriptome of the Asian tiger mosquito, *Aedes albopictus*, to identify candidate transcripts for diapause preparation. BMC Genom. *12*, 619. https://doi.org/10.1186/1471-2164-12-619.
54. King, B., Li, S., Liu, C., Kim, S.J., and Sim, C. (2020). Suppression of glycogen synthase expression reduces glycogen and lipid storage during mosquito overwintering diapause. J. Insect Physiol. *120*, 103971. https://doi.org/10.1016/j.jinsphys.2019.103971.
55. Lehmann, P., Pruisscher, P., Posledovich, D., Carlsson, M., Käkelä, R., Tang, P., Nylin, S., Wheat, C.W., Wiklund, C., and Gotthard, K. (2016). Energy and lipid metabolism during direct and diapause development in a pierid butterfly. J. Exp. Biol. *219*, 3049–3060. https://doi.org/10.1242/jeb.142687.
56. Enriquez, T., and Visser, B. (2023). The importance of fat accumulation and reserves for insect overwintering. Curr. Opin. Insect Sci. *60*, 101118. https://doi.org/10.1016/j.cois.2023.101118.
57. Hao, K., Jarwar, A.R., Ullah, H., Tu, X., Nong, X., and Zhang, Z. (2019). Transcriptome sequencing reveals potential mechanisms of the maternal effect on egg diapause induction of *Locusta migratoria*. Int. J. Mol. Sci. *20*, 1974. https://doi.org/10.3390/ijms20081974.
58. Zhao, J.Y., Zhao, X.T., Sun, J.T., Zou, L.F., Yang, S.X., Han, X., Zhu, W.C., Yin, Q., and Hong, X.Y. (2017). Transcriptome and proteome analyses reveal complex mechanisms of reproductive diapause in the two-spotted spider mite, *Tetranychus urticae*. Insect Mol. Biol. *26*, 215–232. https://doi.org/10.1111/imb.12286.
59. Ma, S.H., Du, X.F., Li, X.J., Xiu, Y., Li, S.Y., and Li, Y.J. (2022). Metabolomic analysis of *Antheraea pernyi* pupa at different deve-lopmental stages. Sci. Seric. (Q.) *48*, 209–215.
60. Yang, C., and Wang, X. (2021). Lysosome biogenesis: Regulation and functions. J. Cell Biol. *220*, e202102001. https://doi.org/10.1083/jcb.202102001.
61. Liu, Y., Hu, D., Lin, Z., Zhou, X., Peng, Z., Yang, B., and Pan, X. (2020). Degradation of biochemical fractions in different temperature of food waste bioevaporation and their contribution to biogenerated heat. J. Clean. Prod. *245*, 118944. https://doi.org/10.1016/j.jclepro.2019.118944.
62. Jarwar, A.R., Hao, K., Bitume, E.V., Ullah, H., Cui, D., Nong, X., Wang, G., Tu, X., and Zhang, Z. (2019). Comparative transcriptomic analysis reveals molecular profiles of central nervous system in maternal diapause induction of *Locusta migratoria*. G3 (Bethesda) *9*, 3287–3296. https://doi.org/10.1534/g3.119.400475.
63. Xu, W.H., Lu, Y.X., and Denlinger, D.L. (2012). Cross-talk between the fat body and brain regulates insect developmental arrest. Proc. Natl. Acad. Sci. USA *109*, 14687–14692. https://doi.org/10.1073/pnas.1212879109.
64. Zhang, X.S., Wang, T., Lin, X.W., Denlinger, D.L., and Xu, W.H. (2017). Reactive oxygen species extend insect life span using components of the insulin-signaling pathway. Proc. Natl. Acad. Sci. USA *114*, E7832–e7840. https://doi.org/10.1073/pnas.1711042114.
65. Lin, X.W., and Xu, W.H. (2016). Hexokinase is a key regulator of energy metabolism and ROS activity in insect lifespan extension. Aging (Albany NY) *8*, 245–259. https://doi.org/10.18632/aging.100885.
66. Abboud, J., Green, S.R., Smolinski, M.B., and Storey, K.B. (2021). Regulation of an important glycolytic enzyme, pyruvate kinase, through phosphorylation in the larvae of a species of freeze-tolerant insect, *Eurosta solidaginis*. Insect Mol. Biol. *30*, 176–187. https://doi.org/10.1111/imb.12687.
67. Durak, R., and Durak, T. (2021). Metabolic response of aphid *Cinara tujafilina* to cold stress. Biology *10*, 1288. https://doi.org/10.3390/biology10121288.
68. Buckner, J.S., Kemp, W.P., and Bosch, J. (2004). Characterization of triacylglycerols from overwintering prepupae of the alfalfa pollinator *Megachile rotundata* (Hymenoptera: Megachilidae). Arch. Insect Biochem. Physiol. *57*, 1–14. https://doi.org/10.1002/arch.20008.
69. Barber, M.C., Price, N.T., and Travers, M.T. (2005). Structure and regulation of acetyl-CoA carboxylase genes of metazoa. Biochim. Biophys. Acta *1733*, 1–28. https://doi.org/10.1016/j.bbalip.2004.12.001.
70. Smith, S., Witkowski, A., and Joshi, A.K. (2003). Structural and functional organization of the animal fatty acid synthase. Prog. Lipid Res. *42*, 289–317. https://doi.org/10.1016/s0163-7827(02)00067-x.
71. Xiang, M., Zhang, H.Z., Jing, X.Y., Wang, M.Q., Mao, J.J., Li, Y.Y., Zang, L.S., and Zhang, L.S. (2021). Sequencing, expression, and functional analyses of four genes related to fatty acid biosynthesis during the diapause process in the female ladybird, *Coccinella septempunctata* L. Front. Physiol. *12*, 706032. https://doi.org/10.3389/fphys.2021.706032.
72. Du, J., Zhao, P., Wang, J., Ma, S., Yao, L., Zhu, X., Yang, X., Zhang, X., Sun, Z., Liang, S., et al. (2022). Pupal Diapause Termination and Transcriptional Response of *Antheraea pernyi* (Lepidoptera: Saturniidae) Triggered by 20-Hydroxyecdysone. Front. Physiol. *13*, 888643. https://doi.org/10.3389/fphys.2022.888643.
73. Xiao, Q.H., He, Z., Wu, R.W., and Zhu, D.H. (2022). Physiological and biochemical differences in diapause and non-diapause pupae of *Sericinus montelus* (Lepidoptera: Papilionidae). Front. Physiol. *13*, 1031654. https://doi.org/10.3389/fphys.2022.1031654.
74. Yaginuma, T., and Yamashita, O. (1999). Oxygen consumption in relation to sorbitol utilization at the termination of diapause in eggs of the silkworm, *Bombyx mori*. J. Insect Physiol. *45*, 621–627. https://doi.org/10.1016/s0022-1910(98)00150-4.
75. Kojić, D., Popović, Ž.D., Orčić, D., Purać, J., Orčić, S., Vukašinović, E.L., Nikolić, T.V., and Blagojević, D.P. (2018). The influence of low temperature and diapause phase on sugar and polyol content in the European corn borer *Ostrinia nubilalis* (Hbn.). J. Insect Physiol. *109*, 107–113. https://doi.org/10.1016/j.jinsphys.2018.07.007.
76. Piper, M.D. (2017). Using artificial diets to understand the nutritional physiology of *Drosophila melanogaster*. Curr. Opin. Insect Sci. *23*, 104–111. https://doi.org/10.1016/j.cois.2017.07.014.
77. King, A.M., and MacRae, T.H. (2015). Insect heat shock proteins during stress and diapause. Annu. Rev. Entomol. *60*, 59–75. https://doi.org/10.1146/annurev-ento-011613-162107.
78. Cui, S.F., Wang, L., Ma, L., Wang, Y.L., Qiu, J.P., Liu, Z.C., and Geng, X.Q. (2019). Comparative transcriptome analyses of adzuki bean weevil (*Callosobruchus chinensis*) response to hypoxia and hypoxia/hypercapnia. Bull. Entomol. Res. *109*, 266–277. https://doi.org/10.1017/S0007485318000512.
79. Lu, Y.X., Zhang, Q., and Xu, W.H. (2014). Global metabolomic analyses of the hemolymph and brain during the initiation, maintenance, and termination of pupal diapause in the cotton bollworm, *Helicoverpa armigera*. PLoS One *9*, e99948. https://doi.org/10.1371/journal.pone.0099948.
80. Purać, J., Kojić, D., Popović, Ž.D., Vukašinović, E., Tiziani, S., Günther, U.L., and Grubor-Lajšić, G. (2015). Metabolomic Analysis of Diapausing

and Noni-diapausing Larvae of the European Corn Borer *Ostrinia nubilalis* (Hbn.) (Lepidoptera: Crambidae). Acta Chim. Slov. *62*, 761–767.

81. Hamasaka, Y., Rieger, D., Parmentier, M.L., Grau, Y., Helfrich-Förster, C., and Nässel, D.R. (2007). Glutamate and its metabotropic receptor in *Drosophila* clock neuron circuits. J. Comp. Neurol. *505*, 32–45. https://doi.org/10.1002/cne.21471.

82. Pascual-Anaya, J., and D'Aniello, S. (2006). Free amino acids in the nervous system of the amphioxus Branchiostoma lanceolatum. A comparative study. Int. J. Biol. Sci. *2*, 87–92. https://doi.org/10.7150/ijbs.2.87.

83. Daniels, R.W., Gelfand, M.V., Collins, C.A., and DiAntonio, A. (2008). Visualizing glutamatergic cell bodies and synapses in *Drosophila* larval and adult CNS. J. Comp. Neurol. *508*, 131–152. https://doi.org/10.1002/cne.21670.

84. Schürmann, F.W., Ottersen, O.P., and Honegger, H.W. (2000). Glutamate-like immunoreactivity marks compartments of the mushroom bodies in the brain of the cricket. J. Comp. Neurol. *418*, 227–239.

85. Collins, B., Kane, E.A., Reeves, D.C., Akabas, M.H., and Blau, J. (2012). Balance of activity between LN(v)s and glutamatergic dorsal clock neurons promotes robust circadian rhythms in *Drosophila*. Neuron *74*, 706–718. https://doi.org/10.1016/j.neuron.2012.02.034.

86. de Azevedo, R.V.D.M., Hansen, C., Chen, K.F., Rosato, E., and Kyriacou, C.P. (2020). Disrupted Glutamate Signaling in *Drosophila* Generates Locomotor Rhythms in Constant Light. Front. Physiol. *11*, 145. https://doi.org/10.3389/fphys.2020.00145.

87. Zimmerman, J.E., Chan, M.T., Lenz, O.T., Keenan, B.T., Maislin, G., and Pack, A.I. (2017). Glutamate Is a Wake-Active Neurotransmitter in *Drosophila melanogaster*. Sleep *40*, zsw046. https://doi.org/10.1093/sleep/zsw046.

88. Love, M.I., Huber, W., and Anders, S. (2014). Moderated estimation of fold change and dispersion for RNA-seq data with DESeq2. Genome Biol. *15*, 550. https://doi.org/10.1186/s13059-014-0550-8.

89. Wen, B., Mei, Z., Zeng, C., and Liu, S. (2017). metaX: a flexible and comprehensive software for processing metabolomics data. BMC Bioinf. *18*, 183. https://doi.org/10.1186/s12859-017-1579-y.

90. Shannon, P., Markiel, A., Ozier, O., Baliga, N.S., Wang, J.T., Ramage, D., Amin, N., Schwikowski, B., and Ideker, T. (2003). Cytoscape: a software environment for integrated models of biomolecular interaction networks. Genome Res. *13*, 2498–2504. https://doi.org/10.1101/gr.1239303.

91. Ye, J., Coulouris, G., Zaretskaya, I., Cutcutache, I., Rozen, S., and Madden, T.L. (2012). Primer-BLAST: a tool to design target-specific primers for polymerase chain reaction. BMC Bioinf. *13*, 134. https://doi.org/10.1186/1471-2105-13-134.

STAR★METHODS

KEY RESOURCES TABLE

REAGENT or RESOURCE	SOURCE	IDENTIFIER
Biological samples		
Adult female *A. chinensis* under normal development	This paper	N/A
Adult female *A. chinensis* under diapause conditions	This paper	N/A
Critical commercial assays		
Triglyceride assay kit	Nanjing Jiancheng Bioengineering Institute	Cat#A110-1-1
TransZol Up Plus RNA Kit	Transgen Biotech	Cat#ER501-01-V2
TransScript One-Step gDNA Removal and cDNA Synthesis SuperMix	Transgen Biotech	Cat#AT311-02
TOROGreen 5G qPCR PreMix	TOROIVD	Cat#QST-200
Deposited data		
Raw RNA sequencing data	This paper	NCBI SRA: PRJNA1154624
Raw and processed metabolomics data	This paper	MetaboLights: MTBLS11731
Supplementary data files	This paper	Available in supplemental information
Oligonucleotides		
All qRT-PCR primers, see Table S1	This paper	N/A
Software and algorithms		
DESeq2	(Love et al., 2014[88])	https://bioconductor.org/packages/DESeq2
NovoMagic platform	Novogene	https://magic.novogene.com
R (Version 3.0.3)	R Core Team	https://www.r-project.org/
metaX	(Wen et al., 2017[89])	https://bioconductor.org/packages/metaX
Cytoscape v3.9.1	(Shannon et al., 2003[90])	https://cytoscape.org/
SPSS 25.0	IBM	https://www.ibm.com/spss
GraphPad Prism 9.4.0	GraphPad Software	https://www.graphpad.com/
NCBI Primer-BLAST	(Ye et al., 2012[91])	https://www.ncbi.nlm.nih.gov/tools/primer-blast/

EXPERIMENTAL MODEL AND STUDY PARTICIPANT DETAILS

No human participants or cell lines were used in this study.

METHOD DETAILS

Insect rearing and micrographic examination

The colony of *A. chinensis* has been maintained in our laboratory for more than three years. Nymphs and adults were reared with Chinese oak silkworm *Antheraea pernyi* pupae under normal developmental conditions of 26°C, with a photoperiod of L16:D8 (16 h light and 8 hours of darkness per 24h), and relative humidity (RH) of 70%.To induce diapause, newly emerged adult females (within 24 hours after eclosion, NE) were exposed to diapause-inducing conditions: 8 hours at 15°C (thermophase) and 16 hours at 5°C (cryophase) with a relative humidity of 70%. Under these conditions, 100% of *A. chinensis* females enter diapause (Figure 1A). Previous studies in our laboratory have shown that after 40 days of diapause induction under these conditions, ovary development in *A. chinensis* female adults arrests, indicating entry into a diapause state (Unpublished, He Weiwei). The diapausing females take about 2 weeks to start oviposition after being transferred to suitable developmental conditions, which is twice as long as the pre-oviposition period of normal developing females. This extended pre-oviposition period, along with arrested ovary development, confirms the diapause status. Adults at the phase of induction (20 days after transferring to diapause-inducing conditions; DI20), phase of initiation (40 days exposing to diapause-inducing conditions, DI40), and phase of maintenance (60 days exposing to diapause-inducing conditions i.e., diapause is maintained for 20 days, DM20), and the newly eclosion adults (NE) were sampled for further experiments. All insects were collected as whole individuals, cleaned, and frozen with liquid nitrogen before being stored at -80°C until analysis. Each treatment was performed with three biological replicates, and each replicate contains one female adult. Morphological

state of *A. chinensis* was visualized using a stereo microscope (Chongguang ZSA0850, Chongqing, China). Abdominal and ovarian examinations were conducted using a digital microscope (Keyence VHX-2000, Osaka, Japan), with abdominal observations performed at 30x magnification and ovarian examinations at 50x magnification. Specifically, dissections were performed at different developmental stages including ND20, ND30, ND40 (non-diapause stages), DI20, DI40 (diapause induction stages), and DM20 (diapause maintenance stage). During these dissections, we observed changes in ovarian morphology and abdominal lipid accumulation, as depicted in Figure 1.

Transcriptome sequencing and data analysis

RNA samples from NE, DI20, DI40, and DM20 stages (3 biological replicates per group) were assessed for quantity and integrity using the RNA Nano 6000 Assay Kit of the Bioanalyzer 2100 system (Agilent Technologies, CA, USA). mRNA was extracted from total RNA by using magnetic beads with Poly-T oligo attachments. The transcriptome was sequenced using second-generation sequencing (Illumina RNA-Seq) technology on the Illumina NovaSeq 6000 platform. Clean data (clean reads) were obtained by removing adapter sequences, reads containing N-bases, and low-quality reads, followed by data analysis-quality control. Quality metrics, including Q20, Q30, and GC content, were calculated to ensure data integrity. Clean reads were assembled into reference sequences using Trinity (v2.6.6). The completeness and accuracy of the transcriptome assembly were evaluated using BUSCO software. This assessment was performed on three different outputs of the assembly process: the initial Trinity assembly (Trinity.fasta), the non-redundant unigene set (unigene. fa), and the final clustered transcripts. BUSCO compares these assemblies against a set of conserved single copy orthologs expected to be present in all insects, providing metrics for assembly quality and completeness. Functional annotation was performed using databases such as Nt (NCBI non-redundant nucleotide sequences), Nr (NCBI non-redundant protein sequences), Pfam (Protein Family), KOG/COG (Clusters of Orthologous Groups of proteins), Swiss-Prot, KO (KEGG Ortholog database), and GO (Gene Ontology). DESeq2 software was used to conduct differential expression analysis, defining DEGs with $|\log2FC| > 1$ and padj < 0.05. GO functions and KEGG pathway analysis of DEGs were performed on the NovoMagic platform (https://magic.novogene.com).

Metabolite profiling analysis

Metabolomic profiles were investigated by Quasi-targeted metabolomics-based on LC-MS/MS. Samples including NE, DI20, DI40, and DM20 were ground with liquid nitrogen and resuspended in prechilled 80% methanol, then centrifuged. The supernatant was diluted to 53% methanol, re-centrifuged, and injected into the LC-MS/MS system. LC-MS/MS analysis was performed using an ExionLC^{TM} AD system coupled with a QTRAP® 6500+ mass spectrometer, using a 20-minute gradient on a Xselect HSS T3 column. Metabolites were identified and quantified by Multiple Reaction Monitoring (MRM) based on an in-house database, with data processed by SCIEX OS Version 1.4. Metabolites were annotated using KEGG, HMDB, and Lipidmaps databases. PCA and PLS-DA were performed using metaX, with univariate analysis (t-test) for statistical significance. Differential metabolites were identified based on VIP > 1, P-value < 0.05, and fold change ≥ 2 or ≤ 0.5. Data visualization included volcano plots, clustering heat maps, and correlation plots using R language packages. For cluster analysis, the optimal number of clusters was determined using the cascadeKM function in the R vegan package, followed by K-means clustering using the kmeans function. The clustering results were visualized using pheatmap package to generate heat maps. Functional analysis of metabolites and pathway enrichment were conducted using the KEGG database, considering pathways with P-value < 0.05 as significantly enriched.

qRT-PCR verification of RNA-Seq

To provide additional support for our RNA-seq findings, we performed quantitative real-time PCR (qRT-PCR) on a subset of differentially expressed genes. These genes represent diverse functional categories relevant to diapause: Dopamine receptor-2 (*DR-2*) and Juvenile hormone acid methyltransferase (*JHAMT*) for neuroendocrine signaling; Phosphoenolpyruvate carboxykinase (*PEPCK*), Acetyl-coenzyme A carboxylase (*ACC*), and Fatty acid synthase (*FAS*) for energy metabolism and lipid synthesis; Timeless (*tim*) for circadian rhythm regulation; and Pyruvate kinase (*PK*) and Hexokinase (*HK*) for glycolysis and energy metabolism. These genes were chosen to provide a comprehensive validation of key pathways implicated in diapause regulation by our transcriptome analysis. The specific primers were designed using NCBI Primer Blast (https://www.ncbi.nlm.nih.gov/tools/primer-blast), and primer sequences are listed in Table S1. The same RNA samples of NE, DI20, DI40 and DM20 for the transcriptomic analysis were used in the RT-qPCR experiment.

Total RNA was extracted from the *A. chinensis* samples according to the protocol of TransZol Up Plus RNA Kit (Transgen, Beijing, China). The concentration of RNA was determined with a NanoDrop spectrophotometer (Thermo Scientific). RNA solution was tenfold diluted and cDNA synthesis was performed using 2000 ng of RNA with the TransScript One-Step gDNA Removal and cDNA Synthesis SuperMix (Transgen, Beijing, China). Briefly, the 20-μL reaction system contained 1 μL of cDNA, 0.8 μL of each specific primer (10 μM), 10 μLof TOROGreen 5G qPCR PreMix (TOROIVD, Shanghai, China), and 7.4 μL of distilled water. The thermocycling conditions were 95°C for 30 s, followed by 40 cycles of 95°C for 10 s and 57–61°C for 20 s. The melting program including 95°C for 10 s, 65°C for 60 s and 97°C for 1 s. The standard reference gene actin was used as an endogenous control to normalize target gene expression levels. Relative expression was analyzed by the $2^{-\Delta\Delta CT}$ method, with three independent biological replicates and three technical replicates.

Triglyceride measurement

To determine the fat accumulation in *A. chinensis* at the diapause induction and maintenance stages, the triglyceride content of 20-35 females in each treatment was measured using Triglycerides Assay Kit (Nanjing Jincheng, A110-1-1, China), by the method of single-agent GPO-PAP. We measured triglyceride levels by first preparing the samples: they were ground with liquid nitrogen, resuspended in prechilled 80% methanol, incubated on ice for 5 minutes, and then centrifuged at 15,000 g for 20 minutes at 4°C. The supernatant was diluted with LC-MS grade water to a final concentration of 53% methanol, transferred to a fresh tube, and re-centrifuged at 15,000 g for 20 minutes at 4°C. For the assay, 2.5 μL of distilled water (for blank), 2.5 μL of standard solution, or 2.5 μL of the prepared sample were added to the respective wells of a 96-well plate, along with 2.5 μL of calibration solution and 250 μL of working reagent. The plate was incubated at 37°C for 10 minutes, and absorbance was measured at 510 nm using a spectrophotometer.

The absorbance values were proportional to the triglyceride content. To calculate the triglyceride concentration in the samples, the absorbance values of the standards were used to create a standard curve. The triglyceride content was then determined using the following formula: Triglyceride content (mmol/g wet weight) = $(A_{sample} - A_{blank}) / (A_{standard} - A_{blank}) \times C_{standard} / (W / V_{extraction})$.

Integrated analysis of transcriptomics and metabolomics

To explore the relationship between transcriptomic and metabolomic profiles, we utilized the heatmap program on the NovoMagic platform, which is based on R software (Version 3.0.3) with ggplot2 and heatmap packages. Given that our transcriptomic (FPKM values) and metabolomic (intensity data) data were derived from separate samples, we conducted the correlation analysis using the mean values for each experimental group (NE, DI20, DI40, and DM20). Specifically, for each gene and metabolite, we calculated the average expression/intensity across the biological replicates within each group. These group means were then used to compute correlations between transcriptomic and metabolomic profiles. Correlations were categorized as negative (coefficient < 0) or positive (coefficient > 0) (Figures S3A–S3C). To clarify the relationship between transcripts and metabolites, correlation analysis was conducted using integrated analysis methods. The correlation analysis between differentially expressed genes and differentially expressed metabolites was conducted using Pearson's statistical method. Correlation coefficients (R^2) and *P*-values for differentially expressed genes and metabolites were calculated. The top ten most strongly correlated transcript-metabolite pairs were selected based on their correlation coefficients, with $|R^2| > 0.8$. Cytoscape (v3.9.1) was used in visualizing the relationship between metabolome and transcriptome (Figures S3D–S3F). To identify the primary biochemical and signaling pathways involving both differentially expressed genes and metabolites, all identified differentially expressed genes and metabolites were mapped to the KEGG pathway database across three different phases of diapause (Figures S3G–S3I).

QUANTIFICATION AND STATISTICAL ANALYSIS

SPSS 25.0 and GraphPad Prism 9.4.0 were used for all data analyses. One-way ANOVA followed by Tukey's LSD tests(α=0.05) was performed to assess the statistical significance of differences in gene expression levels among groups in qPCR experiments. For all other experiments, the Independent-Samples t-test was used to determine the significance of differences between samples. Significance levels are indicated as $^*P<0.05$; $^{**}P<0.01$. The presented values represent the means ± standard error of the mean (SEM).

ADDITIONAL RESOURCES

No additional resources were used in this study.